

PREDICTING CRACK PATTERN ON ARCHIMEDES SCREW RUNNER BLADE OF  
MICRO HYDRO POWER

AHMAD ALIF BIN AHMAD ADAM

A report submitted in partial fulfilment of the requirements for the award of the degree of  
Bachelor of Mechanical Engineering

Faculty of Mechanical Engineering  
UNIVERSITY MALAYSIA PAHANG

JUNE 2013

## **CHAPTER 1**

### **INTRODUCTION**

#### **1.1 Micro Hydro Power**

Hydro power was an output that derived from the water flow energy to be harness for generating useable energy. From the ancient time, people had started to invent a simple hydro system for daily purpose. The ideas of the system eventually move along with the time flow where more brilliant innovation has been made until the advance technology evolution. On this modern day, hydro power has become a huge impact towards the community.

Electricity generation was one of the main reasons on the innovation of hydro power. There were various type of hydro power that been invented with wide range of capacity. For example, the conventional hydroelectric, referring to hydroelectric dam, run-of-the-river hydroelectric, which capture the kinetic energy in river or stream without using the dam, small hydro project which often have no artificial reservoirs, micro hydro project that could consume small output of power at rural area, and pump-storage hydroelectric where it stores water pumped during periods of low demand while released for generation when demand was high.

The micro hydro power was one of the most general hydro powers that had been implemented in the isolated community which live away from the grid. This type of hydro power typically produces up from 4 kW to 100 kW of electricity using the natural flow of the water. The amount of electric power can be enough to supply a home or even small business facility. The component consists inside micro hydro power was a turbine which connected with shaft and small scale generator for transforming the

rotational energy into electric energy. For most of the micro hydropower, there were few common turbine blade type used such as Francis blade, Pelton blade, Kaplan blade, Archimedes blade and etc. the Archimedes blade usually used on low head with high water flow condition. The blade can work efficiently up to on heads as low as 1 meter. The maximum turbine efficiency that can be performed by the Archimedes blade was up to 90 percent as the flow rate increased. Single screws could work on heads up to 8 meters, but above the head level, multiple screws are generally used. Three screw blades were commonly found for this type of hydro power.

As for the conclusion, the Archimedes or screw runner for micro hydro power could consume higher efficiency similar with other type of hydro turbine. Even so the main purpose of the micro hydro turbine was to generate enough amount of electricity for the comfort of certain community that live at rural region in this world.

## **1.2 Archimedes Screw Turbine**

Micro hydropower could consume electricity with higher in turbine efficiency even the turbine type used was low head turbine especially for Archimedes screw turbine. The Archimedean screw pump was one of the oldest hydraulic machines. Today, it was employed in pumping as well as operating in reverse in an energy conversion role for producing useful energy. Despite its age, no consistent theory links the screw's geometry with its mechanical efficiency. The research on the fatigue crack towards the Archimedes blade also still in finding and thus for obtaining the problem solution more of this low head turbine had been implemented at all around the world. Even so, this type of turbine only been implemented at rural area where the community lives were far away from the main grid. This also due to the other used of turbine that produce much more energy compare to Archimedes crew turbine. Thus in order encounters the entire problem related with Archimedes blade, the implementation of the turbine was very important for elaborating the solution for each of the problem that will occur in a normal operating turbine blade.

### 1.3 Problem Statements

The loss of turbine efficiency on the micro hydro power was caused from the crack occur on the turbine blade. The type of turbine blade that used for the micro hydro power was Archimedes screw blade. An analysis has to be made on the fluid flow behavior towards the blade to obtain the prediction of flow where the probability of crack might happen.

### 1.4 Objectives

The objectives for this project were:-

- Developed the CAD model blade using the existing blade dimension.
- To study the behavior of fluid flow acting at the screw runner.
- To predict the crack behavior to the screw runner blade of Micro Hydro Power.

### 1.5 Scopes

In order to accomplish the project objectives, the scopes that need to be listed for the project were as follows,

1. Develop CAD model of the screw runner blade with dimension based from the previous researcher.
2. Meshing the develop CAD model using the ANSYS CFX software.
3. Assuming the fluid medium for the analysis as water in steady state flow, isothermal condition, and isentropic condition.
4. Creating the boundary details for the analysis of the model where the boundary was based on real structure.
5. K epsilon turbulence model will be taken as the solver of the analysis.
6. The flow velocity used is at 2.5 m/s assuming the flow of the river in Malaysia.

## **CHAPTER 2**

### **LITERATURE REVIEW**

#### **2.1 Introduction**

In this chapter we will be discuss about the character and function of Archimedes screw blade and also the design of the blade model. Besides that, the review on fatigue crack prediction analysis on turbomachinery will be further discussed on this chapter.

#### **2.2 Archimedes Screw Blade**

One of the main parts in hydro power was the turbine blade itself. The turbine blade reaction towards water flow creates a rotational motion for the hydro power to generate electricity. There was various type of turbine blade that we can found now days. Archimedes screw blade was one of the turbine blade used in micro hydro power.

Archimedes screw consists of helical blades which surround the central shaft. Back to the old days, the screw blades was a device for lifting water for irrigation and drainage purposes (Rorres et al., 1999) especially from lower to higher area. The blade will be rotated by using a windmill or by manual man power. As the shaft turns, the bottom end of the blade scoops up a volume of water. This water will slide up in the spiral tube, until it finally pours out from the top of the tube and passes into the desired reserve water tank for other daily purpose. The Archimedes screw also had been applied for draining water out of mines. On this modern world, people start to reused and also redesign the blade concept from a pump purpose function to a turbine for generating electricity. On the modern blade design, the screw will be rotated by the water referring

to figure 2.1 as the water was channeled on to the blade channel from higher area to lower area. But the slope involve was not very large since the water flow give enough force to rotate the shaft.

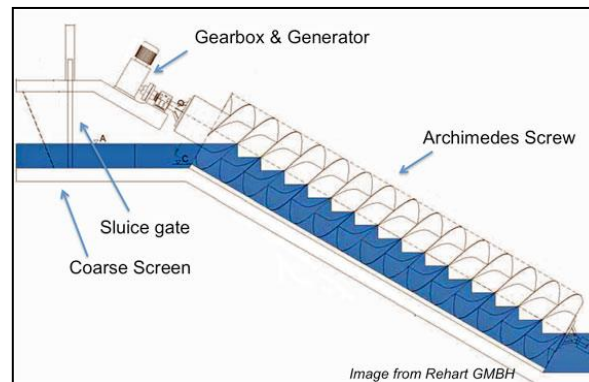


**Figure 2.1:** The structure of Archimedes screw turbine

(Source: Web site [archimedeshydroscrew.com](http://archimedeshydroscrew.com))

Archimedes screw turbines generally was design for heads, in the range of 1 to 5 meters, with flow rates between 0.1 and 50 m<sup>3</sup>/s and should be inclined at an angle, between 22 degree and 33 degree from the horizontal (Stergiopoulou et al., 2012). For greater heads, a cascade of two or more similar energy spiral rotors could give an efficient hydropower solution.

In general, positive output in term of efficiency had been shown by the Archimedes screw. Measurements towards the Archimedean screw as the energy converter showed the effect of inflow water level to diameter, and gave out efficiencies between 79 percent and 84 percent. The high efficiency output gives an interesting alternative for turbines in low head hydropower applications (Muller et al., 2009). The power was generated by the hydrostatic pressure difference and the horizontal screw velocity. The hydrostatic pressure difference between up and down stream acted on the blades which move with the velocity of the upstream water flow. The differential water levels between the up and down stream sides of each blade generate a hydraulic force moving with the screw speed generating a power. Through this power output generated

by the blade, minimum efficiency of the turbine can be obtained from the calculation using efficiency formulation.

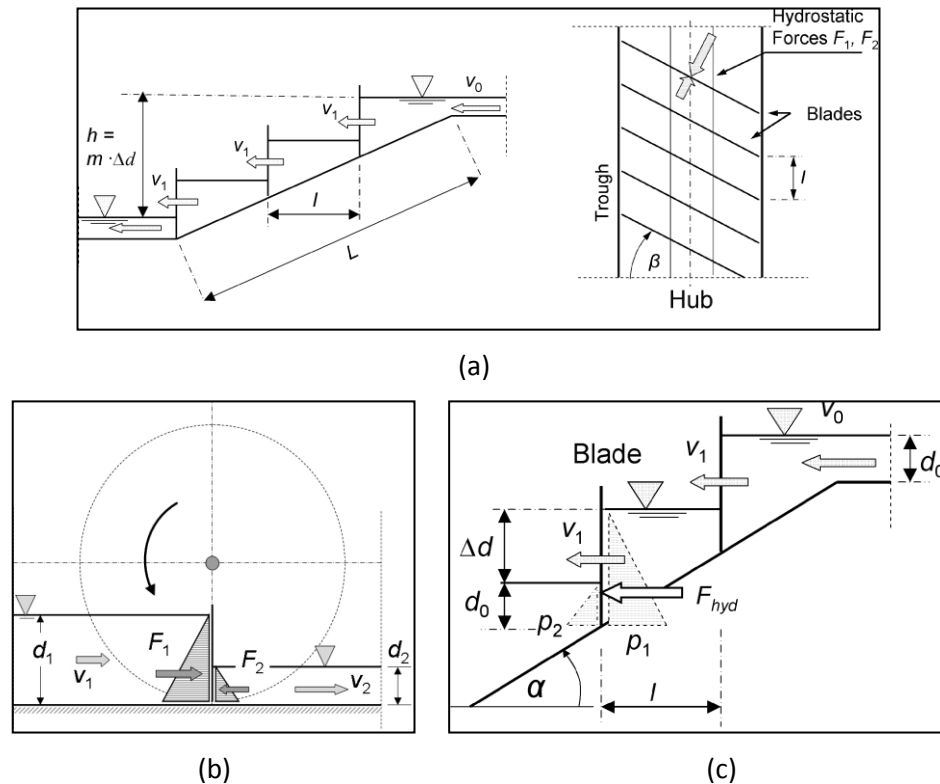


**Figure 2.2:** (a) Idealize Archimedes screw side and plan view (b) Hydrostatic pressure wheel (c) Force acting on individual screw blade

(Source:Geraled Muller et al., 2009)

### 2.2.1 Screw Blade Design

The geometry of helical screw blade was developed through a certain external parameters and also internal parameters. Both parameter lists were outer radius, length, and slope for external and the inner radius, number of blades, and the pitch of the blades for the internal parameters. The external parameters were usually determined by the location of the screw and how much water volume that will be transfer. While, the internal parameters were free to be chosen to optimize the performance of the screw (Rorres et al., 1999).

Referring from figure 2.3, the external and internal parameters were the:

External parameter,

- $R_o$ , radius of the outer cylinder
- $L$ , length of the screw blade
- $K$ , slope of screw blade

Internal parameter,

- $R_i$ , radius of the inner cylinder
- $\Lambda$ , pitch (or period) of on blade
- $N$ , number of blade

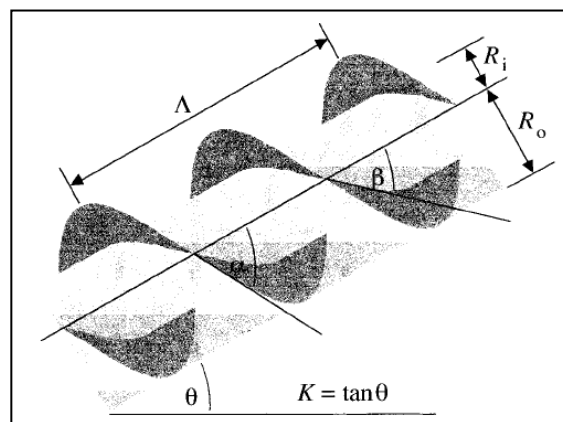


**Figure 2.3:** General external and internal parameter of Archimedes screw

(Source: Chris Rorres et al., 1999)

From the parameter implementation, the similar blade model has been created especially in the turbine blade purpose. In real application of blade design, before manufacturing the real scale turbine blade, modeling need to done for determination dimension of the blade. Figure 2.3 shows the design of screw blade before modeling the blade. The Computer Aided Design was the medium where the blade model will be generated before proceeding with the simulation process.



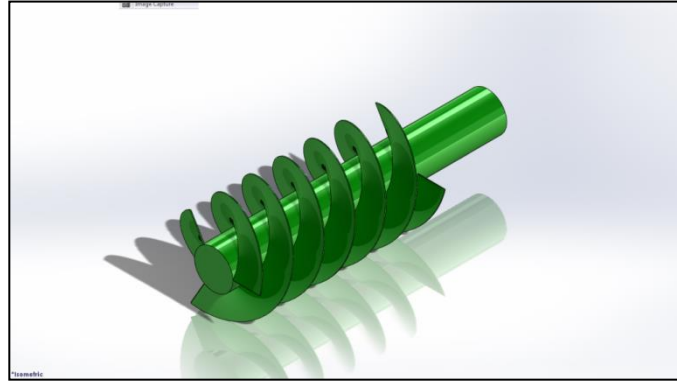


**Figure 2.4:** The CAD model for Archimedes screw

(Source: Solidwork 2012)

The CAD model was generated base from the existent Archimedes screw blade dimension. The benefit of using CAD blade was the model can be put to analysis software for observing the weakness property.

### 2.3 Governing Equation

Computational Fluid Dynamics, CFD was a computer based tool for simulating the behavior of systems involving fluid flow, heat transfer, and other related physical processes. It works by solving the equations of fluid flow which in a special form over a region of interest, with specified conditions on the boundary of that region. The basic governing equation will be involved for the simulations were the mass continuity and momentum equation. The mass was conserved for the fluid was express as in equation 2.1 below.

$$\frac{\partial \rho}{\partial t} + \frac{\partial(\rho u)}{\partial x} + \frac{\partial(\rho v)}{\partial y} + \frac{\partial(\rho w)}{\partial z} = 0 \quad (2.1)$$

Where the fluid velocity at any point in the flow field was described by the local velocity components  $u$ ,  $v$ , and  $w$  which were, in general, functions of location ( $x$ ,  $y$ , and  $z$ ) and time ( $t$ ). The momentum equation was the rate of change of momentum equals with the sum of force acting on the fluid.

The equation of momentum was express as in equation 2.2, 2.3 and 2.4 below for x, y and z direction,

For x momentum equation,

$$\rho \frac{Du}{Dt} = \frac{\partial \sigma_{xx}}{\partial x} + \frac{\partial \tau_{yx}}{\partial y} + \frac{\partial \tau_{zx}}{\partial z} + \sum F_x^{bodyforce} \quad (2.2)$$

For y momentum equation,

$$\rho \frac{Du}{Dt} = \frac{\partial \sigma_{xy}}{\partial x} + \frac{\partial \tau_{yy}}{\partial y} + \frac{\partial \tau_{zy}}{\partial z} + \sum F_y^{bodyforce} \quad (2.3)$$

For z momentum equation,

$$\rho \frac{Du}{Dt} = \frac{\partial \sigma_{xz}}{\partial x} + \frac{\partial \tau_{yx}}{\partial y} + \frac{\partial \tau_{zz}}{\partial z} + \sum F_z^{bodyforce} \quad (2.4)$$

The normal stresses  $\sigma_{xx}$ ,  $\sigma_{yy}$  and  $\sigma_{zz}$  were due to the combination of pressure and normal viscous stress components  $\tau_{xx}$ ,  $\tau_{yy}$  and  $\tau_{zz}$  acting perpendicular to the control volume. The expression of  $\rho \frac{Du}{Dt}$  was not implement. This was due to the simulation flow was assumed to be in steady condition. The energy equation was not included for the simulation due to no heat transfer process and also no change in temperature occurred. The flow was stated as in isentropic and isothermal boundary condition.

There were various type of turbulence model existed for solving the computational fluid problem, one of the common turbulence model was the k-Epsilon model. The equation of the model as follows,

For turbulent kinetic energy, k,

$$\frac{\delta}{\delta t}(\rho k) + \frac{\delta}{\delta x_i}(\rho k u_i) = \frac{\delta}{\delta x_i} \left[ \left( \mu + \frac{\mu t}{\mu k} \right) \right] \frac{\delta k}{\delta x_i} + Pk + Pb - \rho \varepsilon - YM + Sk \quad (2.5)$$

For dissipation energy,  $\varepsilon$  epsilon,

$$\frac{\delta}{\delta t}(\rho\varepsilon) + \frac{\delta}{\delta x_i}(\rho\varepsilon u_i) = \frac{\delta}{\delta x_j} \left[ \left( \mu + \frac{\mu t}{\sigma\varepsilon} \right) \frac{\delta\varepsilon}{\delta x_j} \right] + C_1\varepsilon \frac{\varepsilon}{k} (Pk + C_3\varepsilon Pb) - C_2\varepsilon\rho \frac{\varepsilon^2}{k} + S\varepsilon \quad (2.6)$$

The turbulence viscosity is modeled as,

$$\mu t = \rho C\mu \frac{k^2}{\varepsilon} \quad (2.7)$$

The production of k is modeled as,

$$Pk = \mu t S^2 \quad (2.8)$$

S is the modulus of the mean rate-of-strain tensor, defined as,

$$S = \sqrt{2S_{ij}S_{ij}} \quad (2.9)$$

The model constant for k-  $\varepsilon$

$$C_1\varepsilon = 1.44 \quad C_2\varepsilon = 1.92 \quad C\mu = 0.09 \quad \sigma k = 1.0 \quad \sigma\varepsilon = 1.3$$

The reason of listing the k-epsilon turbulence model was due the consideration of the blade where the flow was in turbulent, compressible fluid, the blade was set to be unmoving (Torshizi et al., 2008) and addition of rotational component to axial velocity of the water flow to count the blade rotation.

## 2.4 Blade Optimum Rotation

The Archimedes screw blade consists of helical structure which counts in number of the helical rotation. The number of blade rotation was considered for obtaining higher value of efficiency. Based from the previous research done, the higher number of blade turns was desirable in order to maintain the high efficiency of the turbine (Muller et al., 2009). 14 helical turns will give up higher turbine efficiency with low slope angle and also head value as shown in figure 2.5.

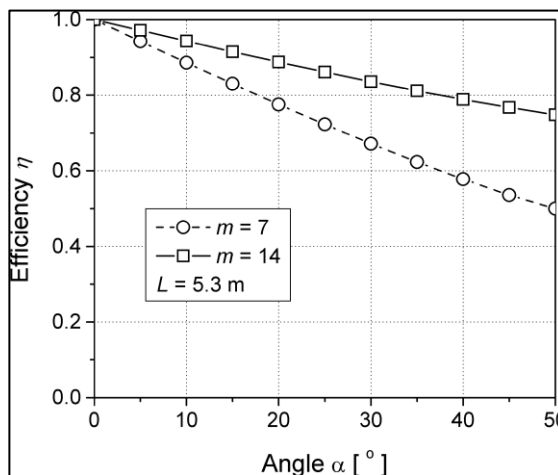


**Figure 2.5:** The theoretical efficiency as function of slope angle and number of helical turns

(Source: Gerald Muller et al., 2009)

Thus, the blade model used for the analysis will be consisting of 14 numbers of helical turns, 23.58° slope angle and head of 2.24 meters. The fixed value was taken for obtaining the optimum analysis result later.

## 2.5 Fatigue Crack

Fatigue occurrence was a general problem that usually occurs in turbine blade. The fatigue cracks normally represent in regions that have a metallurgical or structural discontinuity and were subjected to higher stresses (source: Flores et al., 2011). The concept of local strains and stresses were the common approach for predicting the crack initiation growth in a structure to fatigue loads. In the most of hydro power, the turbines blade had been operated for decades. Due to the current operating conditions, the blade structure was now become different from the original design specified. These operations cause vibrations and some have presented cracks in the runners produced by fatigue.

Lots of research has been done on the fatigue crack analysis of turbine blade. Each of the research had implemented various kind of method on identifying the crack behavior towards the turbine especially at the runner blade. The runner blade of a

turbine was the most critical structure and usually expose to environment or even to the medium which help in giving the motion to the turbine runner blade such as air, water and etc. Most of the research done for fatigue crack analysis on hydropower was more focus on the normal used turbine such as Francis turbine. Most of the cases studied on the stress analysis of the turbine runner. The crack occurrence will be detected base on the numerical method. The result obtains from simulation of Francis runner blade show the zone with high stress was situated at the transition between the blade and the crown on the outlet side (Source: Saeed et al., 2010). Figure 2.6 shows the appearance of fatigue crack on the Francis turbine through experiment and also simulation.

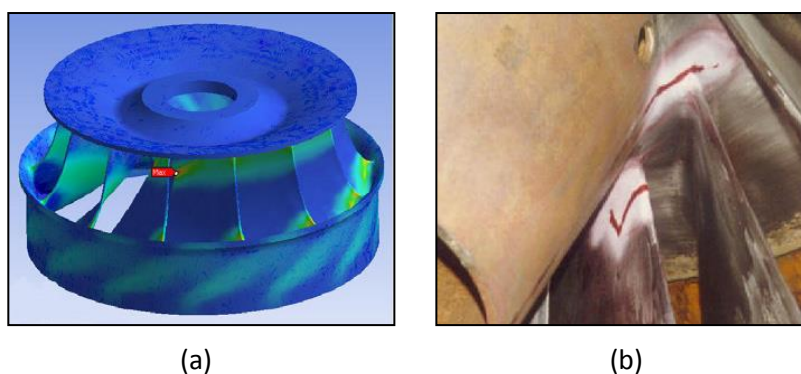


**Figure 2.6:** (a) Analysis using of the Francis turbine using computer simulation (b) Real image of the crack occurrence at the Francis turbine

(Source: R.A. Saeed et al., 2010)

Other research done on the fatigue crack analysis was based on the crack initiation life was done by Flores et al., (2012). Based from the research, the model of the runner was constructed to perform the modal and the static stress analysis using the commercial software. The static stress of the runner was calculated due to the load effect in the operational conditions cause by the centrifugal forces and the fluids static pressure. The calculation of the dynamical stress was done for blades passing the guide vanes. Thus, from the all the gather calculated values, the estimation of the cracking initiation growth on the runner was obtain where the dynamical stress was maximum at the blade near to the bend which located close to the runner exist (Source: Flores et al., 2012). From this situation, the crack occurrence will exceed as the turbine operate at the maximum stress condition.

Besides that, there are also researches of fatigue crack on the wind turbine and also gas turbine type. The crack analysis concept was still similar with the hydro turbine type but different in medium. Example for wind turbine type, the fatigue crack analysis will be made on the real wind turbine blade. The turbine blade was already in operation and crack had been occurring at the joining zone of the blade and the root as shown on figure 2.7. Evaluation on the crack occurrence will be added with simulation on the stress acted at the crack section. From here, the maximum stress can be obtain and explanation of the fatigue crack was made where at a certain point of the blade, there was weak point that lead to the crack initiation (Source: Marin et al., 2008). Besides that the condition of the blade expose to high wind intensity influence the stress acted at the critical zone of the blade.

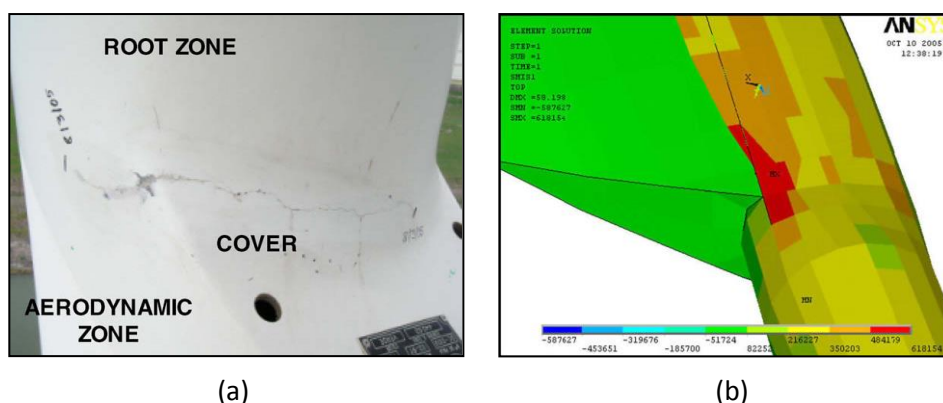


**Figure 2.7:** (a) The crack propagation on the wind turbine blade (b) The simulation of the pressure distribution on the wind turbine blade

(Source: J.C.Marin et al., 2008)

For the gas turbine type example, the fatigue crack analysis was done from the existing blade that already in the state of crack initiation. The crack that occurs at the blade will be observed first on the microstructure view for obtaining the explanation from the crack structure behavior where due to alternative loading of the blade during the rotation, the crack propagation occur by fatigue and resulting fracture of the blade. Later, model of the blade was generated for the computer analysis using the simulation as shown in figure 2.8. Vibration of the blade was simulated as the result where high vibration causes the blade to achieve the fatigue stage during the blade rotation. From

the fatigue analysis made from the research, in resonance condition, the nominal stress impose on the blade exceed the normal stress and this lead to exceeding of stress against the endurance limit of the material where it can lead to failure on the blade structure (Source: S.E. Moussavi Torshizi et.al.2009).

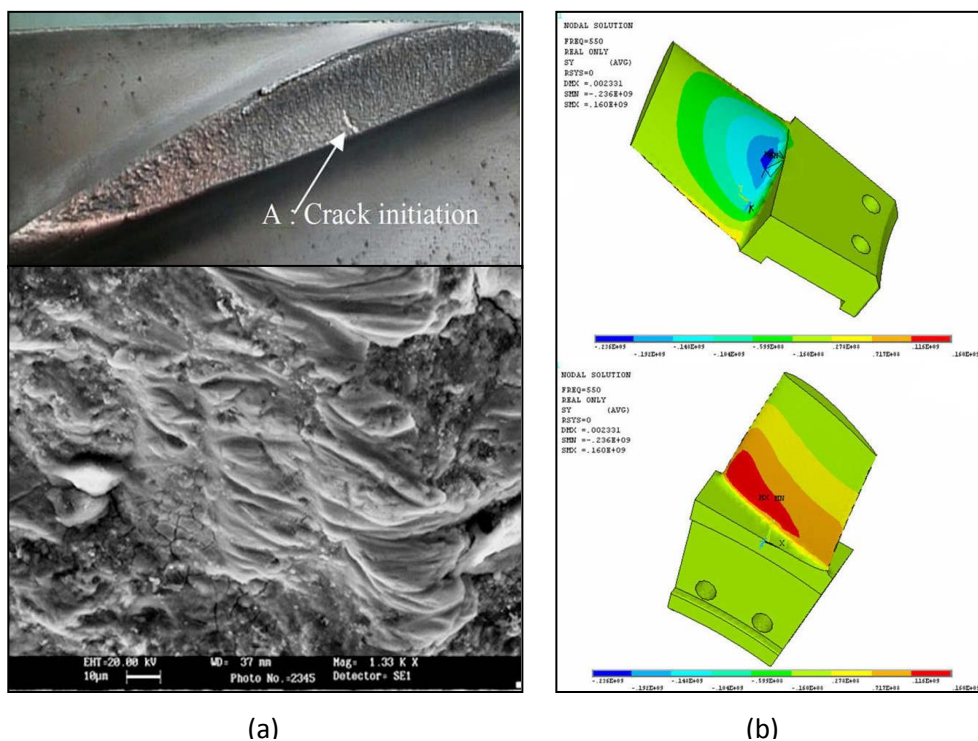


**Figure 2.8:** (a) The microstructure of the crack initiation (b) the distribution of stress at the gas turbine blade

(Source: S.E. Moussavi Torshizi et.al.2009)

Even though there were lots of crack researches on turbine runner, yet there was no research on crack had been done for the screw runner blade for micro hydro power turbine. In this project, the analysis was more towards predicting the crack due to erosion and sedimentation in the river bead.

## 2.6 Crack Pattern Simulation

For the project, the ANSYS CFX was used as the base for simulation. The ANSYS simulation helps by providing the all the detail for the analysis of the crack on blade. In figure 2.9 (a) and (b) shows the velocity movements of water flow in Francis turbine and the absolute pressure acted on the turbine structure.

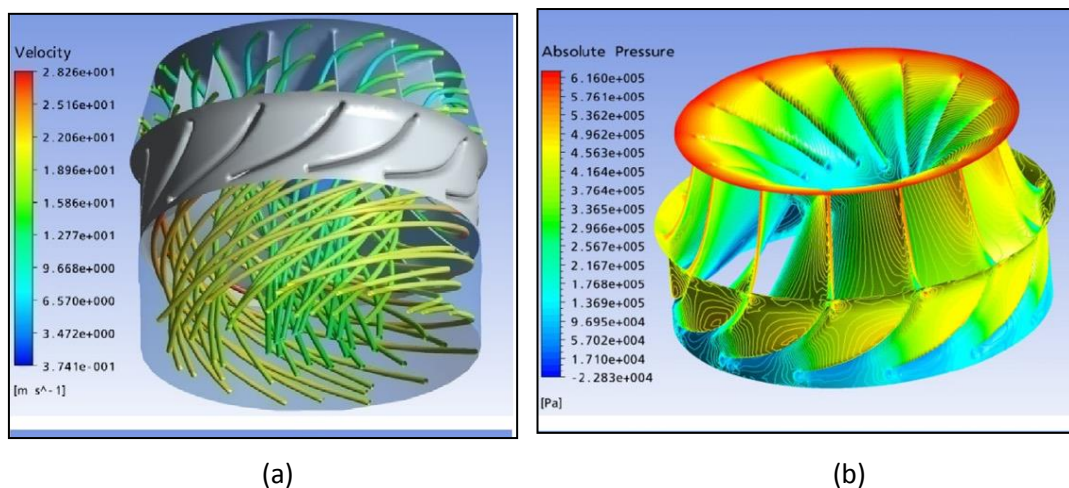


**Figure 2.9:** (a) The fluid flow visual from ANSYS on Francis turbine (b) The pressure distribution from ANSYS on Francis turbine

(Source: R.A. Saeed et.al.2010)

The CFX code had also been validated in predicting performance result based on global parameter (Source: Prasad et al., 2012). For the crack analysis, the simulation will be focus more on the stress analysis of the screw runner blade and the analysis of fluid flow through screw runner blade.

Besides that, the pressure distribution causes by the fluid flow will be observed for predicting the crack initiation on the screw runner blade. The considered parameters for the simulation were,



- Coefficient of pressure,  $C_p$

$$C_p = \frac{\Delta P}{\frac{1}{2} \rho W_2^2} \quad (2.10)$$

Where,  $\Delta P$  = Pressure difference (Pa)

$\rho$  = Mass density of water ( $\text{Kg/m}^3$ )

$W$  = Blade surface velocity (m/s)

The boundary condition was compulsory for the analysis process in ANSYS CFX. The setup of boundary condition will consist of inlet and outlet condition. For the fluid flow cases, the inlet boundary will be the velocity inlet where water entering the turbine and leaving at the outlet boundary. The top wall, bottom wall and side wall will remain constant in velocity,  $V=0$ . Figure 2.10 shows the boundary condition in ANSYS CFX with the assumption of rectangular shape flow tunnel.

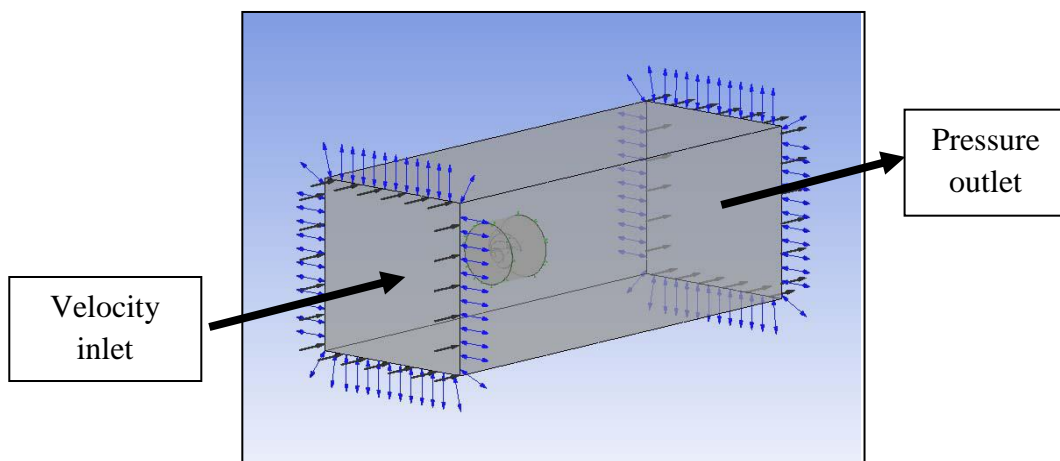


**Figure 2.10:** Imaginary space on ANSYS

(Source: Yoon Kee Kim et al., 2008)

The imaginary part of the for the analysis will be determine whether in rectangular or cylinder or other desired shape that can be apply inside the ANSYS software.

## 2.7 Velocity of Pahang River

The mean velocity of Pahang River specifically at Pekan area was 2.46667 m/s as shown on table 2.2 below. The velocity value was used for the simulation of the screw blade.

**Table 2.2:** Data Obtained Regarding Velocity of Pahang River

River part		Velocity of Pahang River (m/s)								Mean
		Jan	Feb	March	April	May	June	July	Aug	
Pahang river (Temerloh)	Minimum	2.1	2.3	2.6	2.3	2.1	2.3	2.6	2.1	2.3
	Mean	2.3	2.5	2.5	2.5	2.3	2.5	2.5	2.3	2.425
	Maximum	2.5	2.7	2.4	2.7	2.5	2.7	2.4	2.5	2.55
Jelai river (Kuala Medang)	Minimum	2.3	2.3	2.2	2.3	2.3	2.6	2.1	2.3	2.3
	Mean	2.5	2.5	2.4	2.5	2.5	2.5	2.3	2.5	2.4625
	Maximum	2.7	2.7	2.6	2.7	2.7	2.4	2.5	2.7	2.625
Pahang river (Pekan)	Minimum	2.3	2.6	2.3	2.1	2.6	2.3	-	-	2.36667
	Mean	2.5	2.5	2.5	2.3	2.5	2.5	-	-	<b>2.46667</b>
	Maximum	2.7	2.4	2.7	2.5	2.4	2.7	-	-	2.56667

(Source: Department of Irrigation and Drainage Malaysia)

## 2.8 Conclusion on the Literature Review

Based from the literature research on the turbine blade for the crack analysis, it can be concluded that the project result will be on the prediction of crack on the screw runner blade.

## **CHAPTER 3**

### **METHODOLOGY**

#### **3.1 Introduction**

In this chapter, the information written will be covered more towards the method used for this project work. The method used for obtaining the result and conclusion for this project was based from the previous research that had been made by other people. The basic method that we can take from the previous method was development of the design for the model which for this case was the blade model. Most of the research made used Computer Aided Design, CAD model for interpreting their model design. Each of the design contains their own dimension from simple calculation for giving accurate design. Later the CAD model will be transferred to the analysis software for further investigation. Since the analysis contains the interaction with fluid behavior, ANSYS CFX software was used for this type of analysis. Inside the software, it contains various type of function for obtaining the desired result. Simulation on the fluid behavior also can be obtained from this advance numerical system.

#### **3.2 Flow Chart**

The flow chart in figure 3.1 shows the sequence of method used for the project progress. For the Semester 1, Final Year Project, the progress set up was more likely towards the design stage of the screw blade before proceeding with simulation. The design stage covers from the rough sketch of the screw blade until producing the CAD model. The expected crack design was determine with the help from literature review reading and also supervisor advice. After the CAD model completed, the model was transfer into the analysis software, ANSYS to be mesh. The meshing condition also was

also according to the idea from literature review reading together with supervisor advice. If the model fails on the meshing process, it means there was an error that occurred on the CAD model and correction towards the blade model will be done. On the same time also each main component that needed to be inserted inside the ANSYS later will be determined as expected parameters, boundary condition and type of meshing.

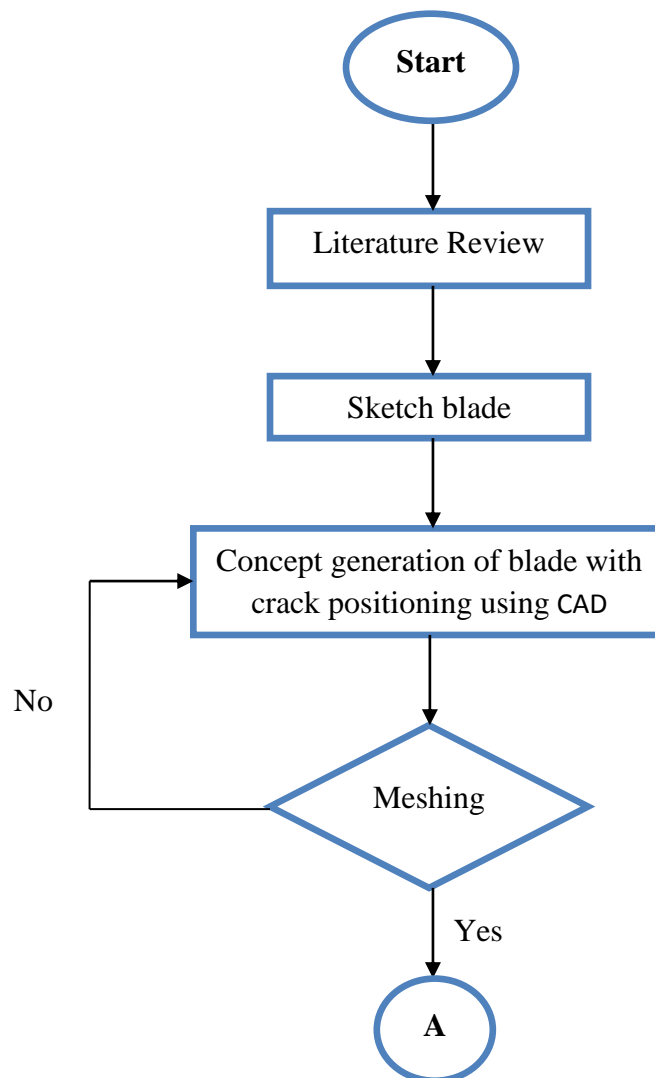


**Figure 3.1:** Flow chart for Semester 1 FYP progress

For figure 3.2 shows the Semester 2, Final Year Project, the progress was more likely towards analysis stage. From the expected parameters, boundary condition and also turbulence model, the most suitable component was chosen for the whole analysis

process. The analysis result will be taken for conclusion making. Final report writing will finish for this final year project analysis and also final presentation.

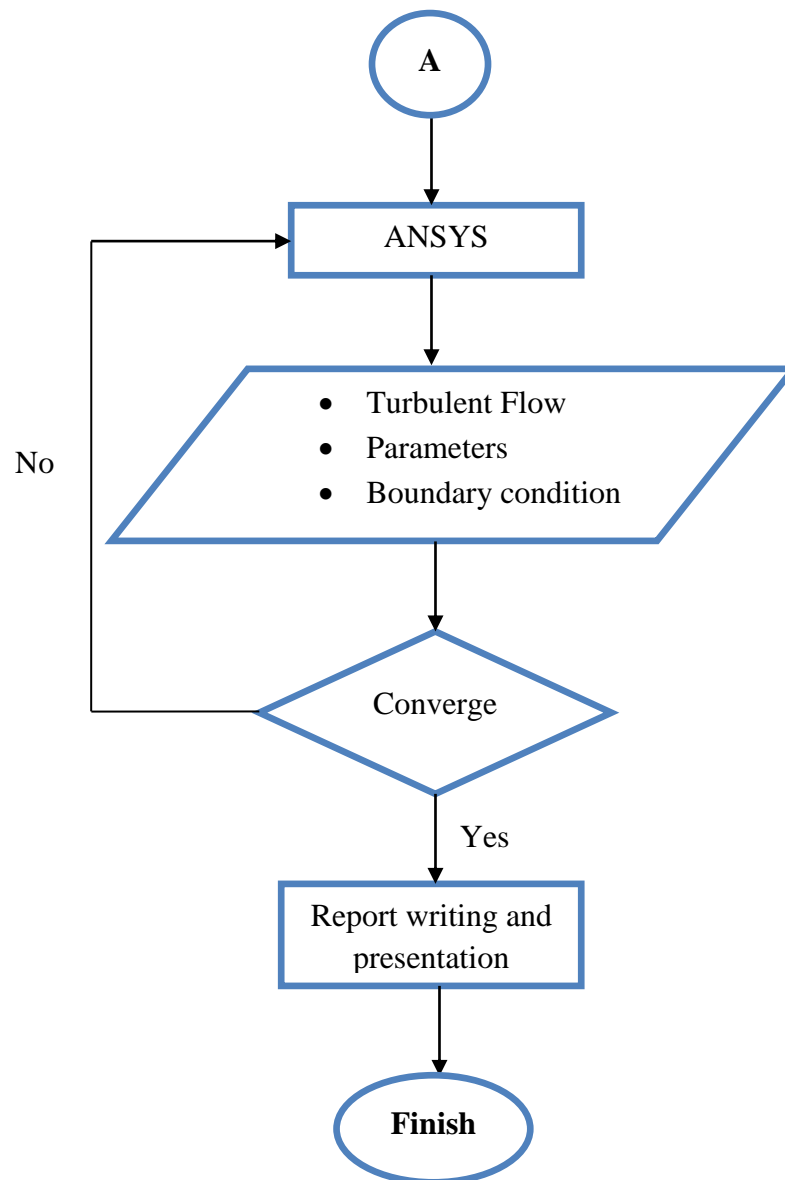
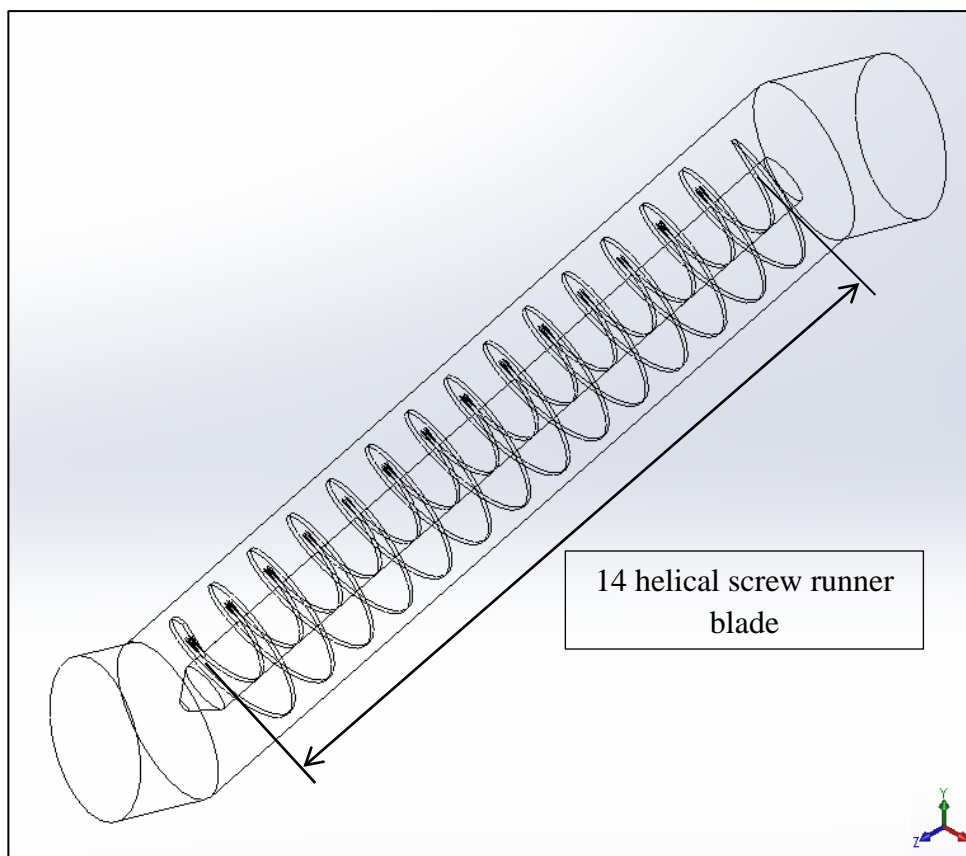


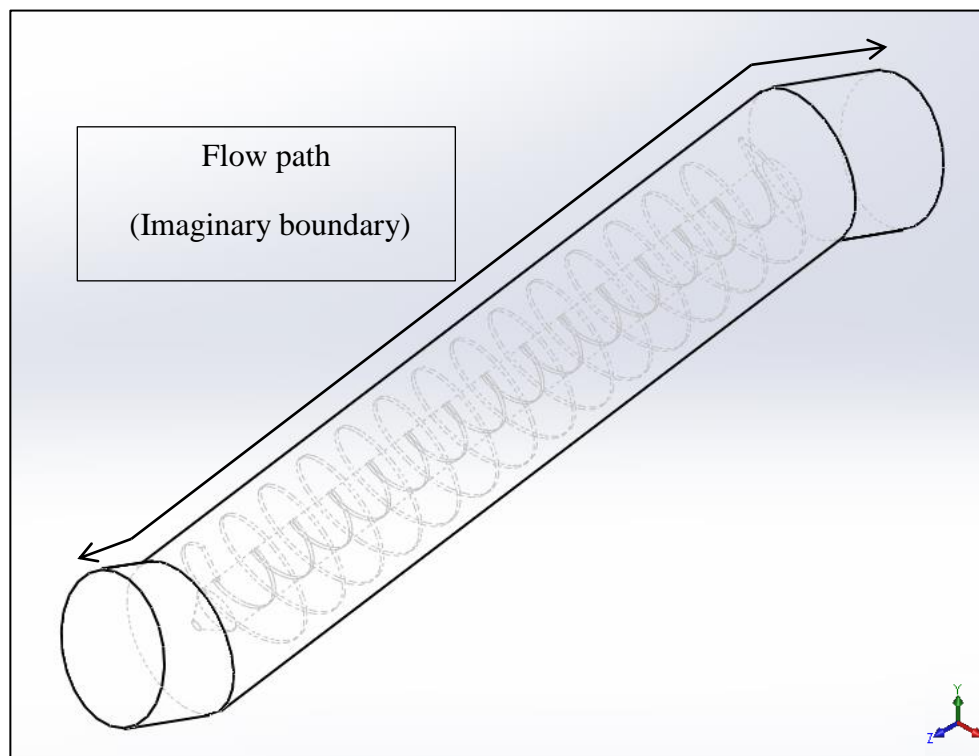
**Figure 3.2:** Flow chart for Semester 2 FYP progress

### 3.3 CAD Modeling

For the modeling stage, SolidWork software was used for the screw blade Computer Aided Design modeling. SolidWork was the bench mark software for CAD model generation where the software consists of multiple choice of instruction suitable for producing model. For the project blade design, the entire screw blades models were generated according to the concept sketch. 3-dimensional model of the screw blade and water path was made using SolidWork software. As the screw blade only half immersed in the water, the rotation motion of the blade was used for assuming the condition where the all the blade structure was immersed in the water. Thus, full cylindrical water path with the blade inside the path was made as figure 3.3 (a) and (b).



(a)



(b)

**Figure 3.3:** (a) Wireframe view and (b) Hidden line visible view of the screw runner blade with flow path on SolidWork

(Source: SolidWork 2012)

Based from figure 3.5 (a), it shows the CAD model design of the screw blade located inside the flow path. The dimension used for the screw blade model was shown in table 3.1 below.

**Table 3.1:** Dimension of the screw runner blade

Description	Detailed value
Length, L (m)	5.32
Outer Radius, $R_o$ (m)	0.52
Inner Radius, $R_i$ (m)	0.50
Pitch, $\Lambda$ (m)	0.38
Number of blade, N	14 revolution

For figure 3.5 (b) shows the CAD model of the flow path of the screw runner blade. The dimension for the flow path model was shown as in table 3.2 below.

**Table 3.2:** Dimension of the flow path

Description	Detailed value
Length, L (m)	6.8
Radius, (m)	0.6
Slope, K (degree)	23.58°
Head, H (m)	2.24

### 3.4 Meshing (ANSYS CFX)

The meshing process needed to be done for detecting whether the CAD model was good or vice versa. The mesh in ANSYS consists of medium, small and fine mesh. As for the blade model, fine mesh will be used for the process. The reason on using the fine mesh was to increase the accuracy in the analysis result later.

Fine mesh was selected for the meshing of screw blade and water path. The smaller mesh sizes for the geometry in the water flow are used to obtain more accurate results. The mesh size at the blade structure was more focus in order to get the more accurate result value after the simulation of the fluid flow. Figure 3.4 shows the mesh result of the exported CAD model of the flow path with screw runner blade based on tetrahedral grids.



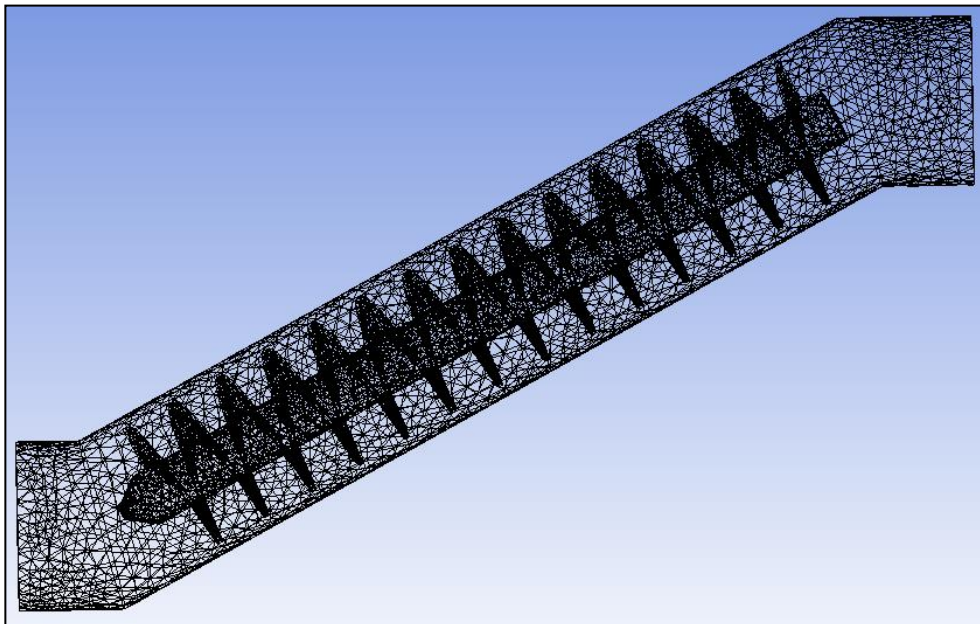


**Figure 3.4:** Mesh structure of the flow path and screw runner blade

(Source: ANSYS CFD)

Table 3.3 shows the detailed values of mesh obtain from the ANSYS software in form of nodes and element of the mesh structure.

**Table 3.3:** Meshing detail of the flow path and screw runner blade

Description	Detailed value
Number of nodes	27739
Number of elements	136430 (tetrahedral)

### 3.5 Simulation

The simulation will be done using ANSYS CFX. The reason of using the ANSYS software because the CFX code itself was validate for turbine application by many investigations. It was very difficult to obtained pressure and velocity distribution in experimental process compared to numerical solver method. We could set up the

parameter and also the boundary condition similar as in real situation before running the simulation.

### 3.5.1 Boundary Condition

The setup of the simulation begins with creation of the boundaries and the default domain for the screw runner model. Figure 3.5 shows the setup of the fluid domain and also the boundary detail for the simulation. The inlet boundary was set as velocity inlet while the outlet boundary was set as opening.

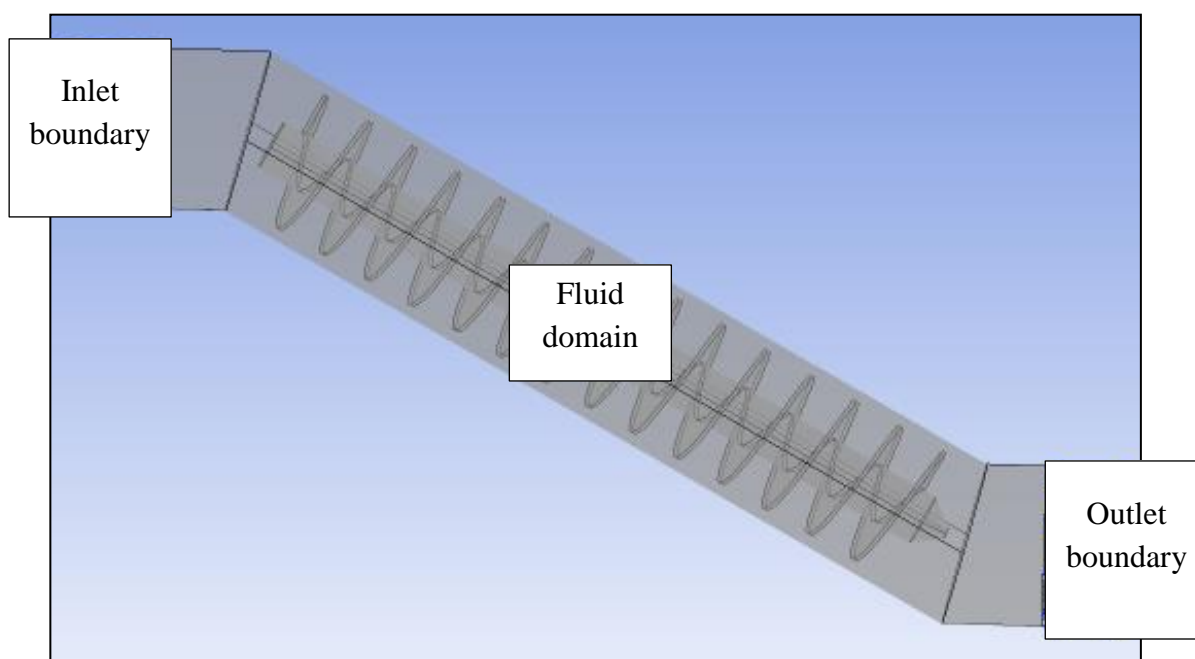


**Figure 3.5:** The boundary condition setup for the simulation

(Source: ANSYS CFD)

Table 3.4 shows the fluid domain detailed of the flow path with screw runner blade for the simulation.

Fluid domain,

**Table 3.4:** Default domain details

Description	Detailed Values
Fluid Type Domain	Water
Water density (kg/m <sup>3</sup> )	1000
Water dynamic viscosity (kg/m-s)	0.001
Opening pressure (Pa)	101, 300
Heat transfer option	Isothermal ( 25°C )

### 3.5.2 Imaginary Boundary

The imaginary boundary for the screw runner turbine was base from the cylindrical tube with the screw blade situated at the incline position on the water flow path. The figure 3.6 shows the imaginary water flow path for the turbine and also boundary condition set for the simulation process. Table 3.2 shows the detailed dimension of the follow path which was the imaginary boundary for the simulation.

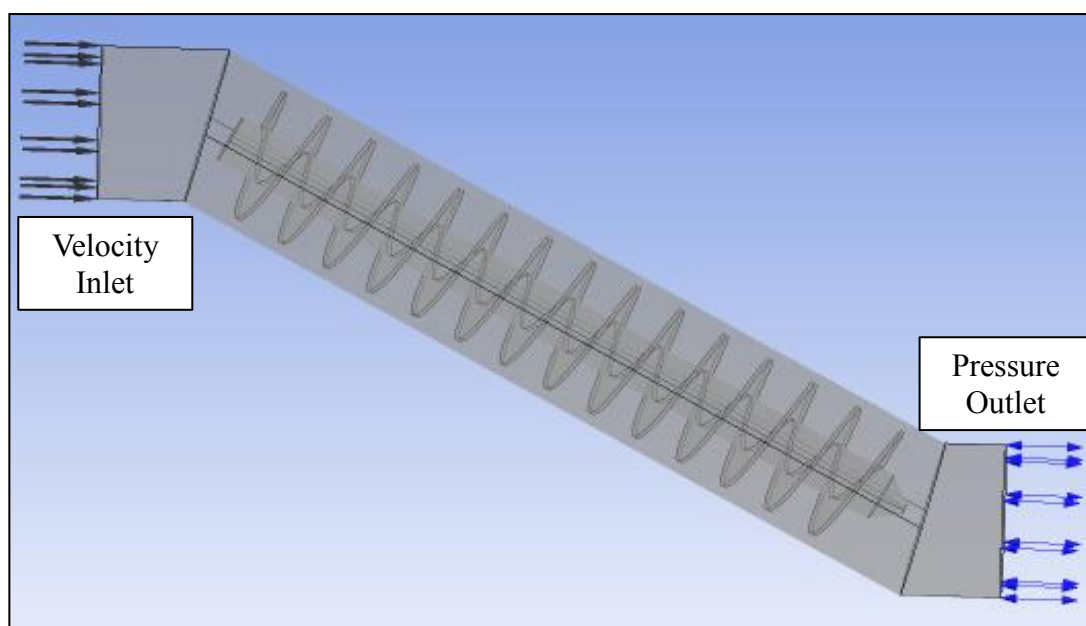


**Figure 3.6:** The imaginary boundary for water flow inlet and outlet

(Source: ANSYS CFD)

The boundary conditions used for the simulation set up were velocity inlet and pressure outlet. Table 3.5 below shows the variables that were selected for each of the boundaries.

**Table 3.5:** Inlet boundary and Outlet boundary details

Description	Detailed Values
<u>Velocity Inlet</u>	
Boundary Type	Inlet
Boundary Detailed	Normal Speed, 2.5 m/s (River Flow Velocity)
<u>Pressure Outlet</u>	
Boundary Type	Opening
Boundary Detailed	Entrainment with Relative Pressure 0 Pa (Opening Pressure)

### 3.6 Simulation of the Flow

The simulation of the flow in boundary condition under turbulent model K- $\epsilon$  was shown in figure 3.9 below.

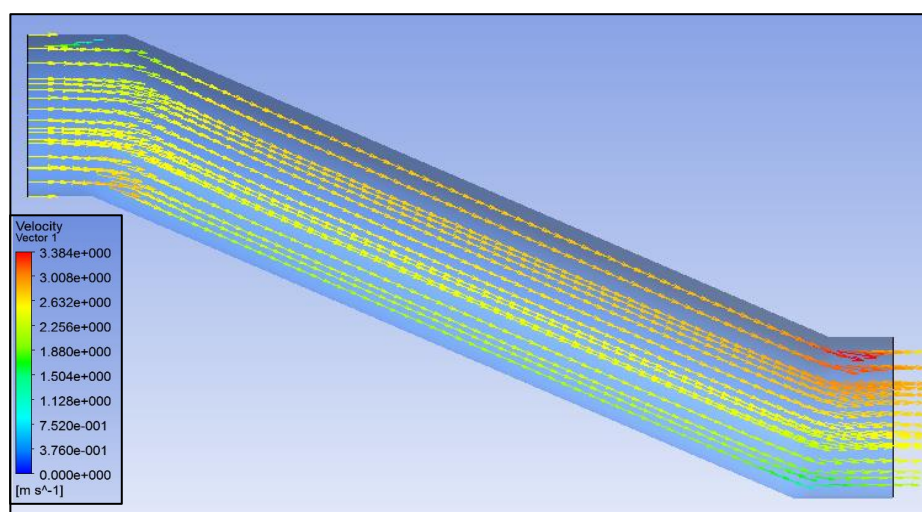


**Figure 3.7:** Velocity vector view at the flow path

(Source: ANSYS CFD-Post result)

Figure 3.7 shows the graph of velocity versus the flow path distance plotted from the simulation result.

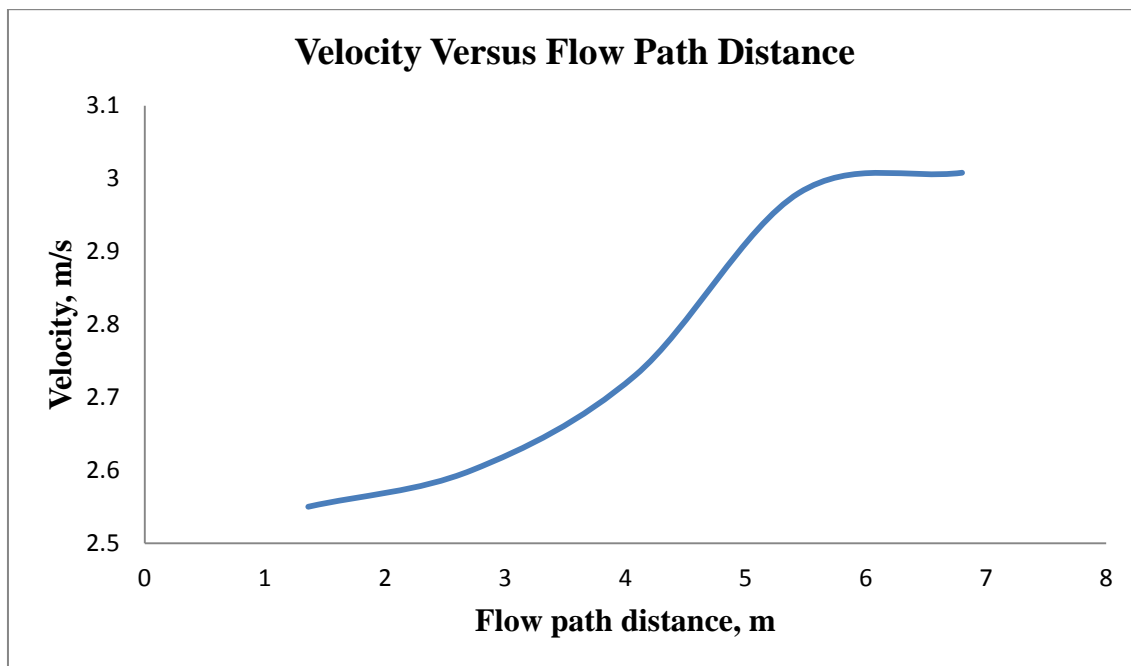


**Figure 3.8:** Graph of velocity versus flow path distance

## **CHAPTER 4**

### **RESULT AND DISCUSSION**

#### **4.1 Introduction**

In this chapter we will be discuss in detail about the computational flow modeling using ANSYS CFX. The flow simulation was based from the screw runner blade turbine inside the flow path which similar with the real situation. The 3-Dimensional flow of fluid was numerically analyzed using the appropriate continuity equation. The result of the simulation was based from the velocity distribution, velocity vector and pressure distribution produce at the blade structure. The coefficient of pressure value of the blade also was taken from the simulation result.

#### **4.2 Result of Velocity Pattern**

The result obtained from the simulation was observed in various views. The first observation made for the simulation was based on the velocity of the water flow. The velocity flow was plotted in plane structure along the flow path and also viewed in vector. The velocity vector reassembles the velocity of the water flow and also the flow pattern along the model. Figure 4.1 shows the velocity distribution acted on the flow pattern and figure 4.2 shows the velocity vector of the water flow through the flow path.

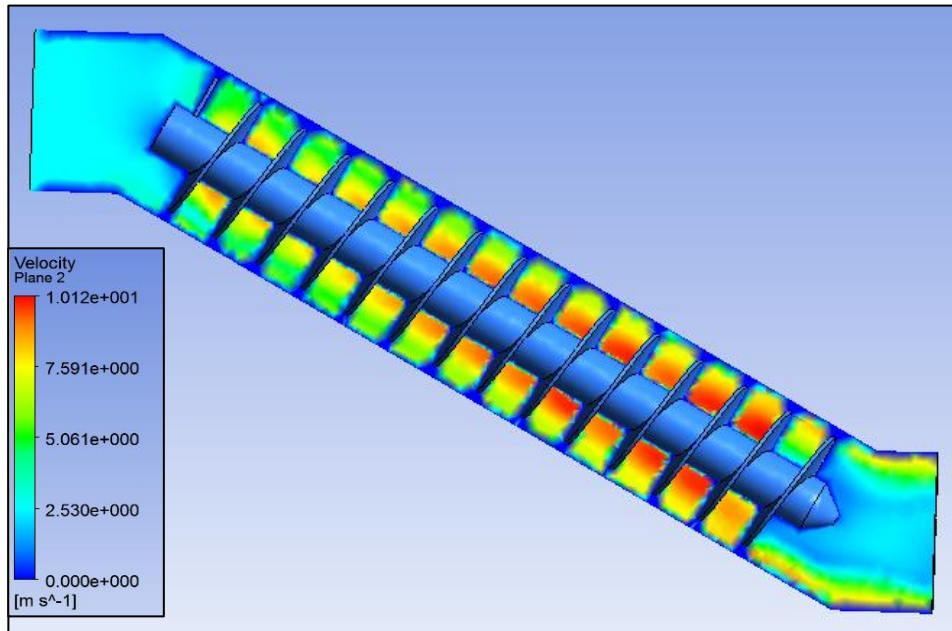


**Figure 4.1:** Velocity distribution plane view at the flow path

(Source: ANSYS CFD-Post result)

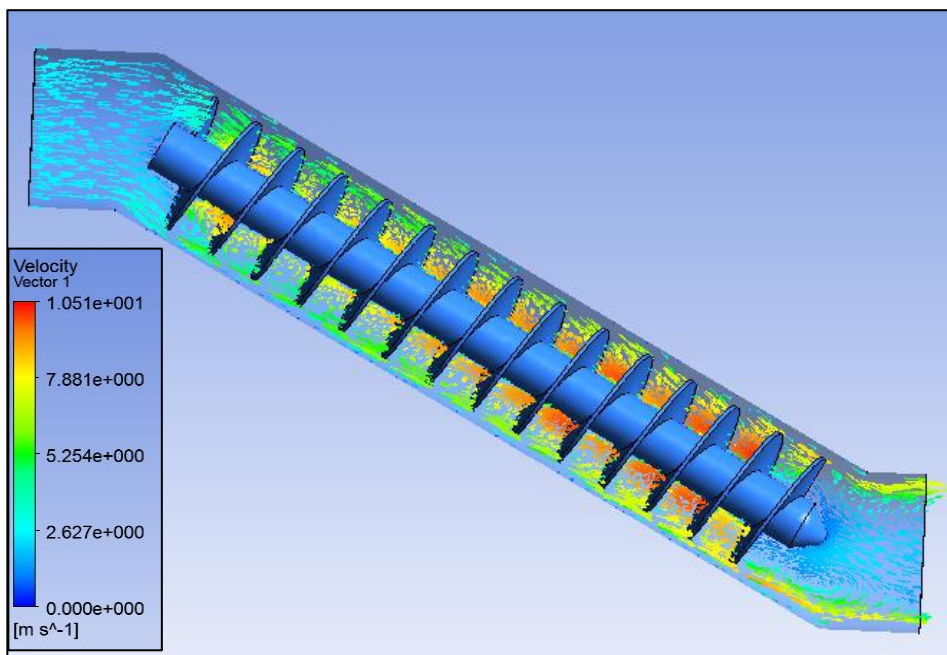


**Figure 4.2:** Velocity vector view at the flow path

(Source: ANSYS CFD-Post result)

### 4.3 Result of Pressure Pattern

The second result observation was in form of pressure pattern. The pressure distribution was observed at the desired location which at the screw blade structure. Figure 4.3 shows the pressure distribution pattern produce from the simulation. The pattern was viewed in contour pattern. While in figure 4.4, the plane viewed was applied for observing the pressure distribution along the flow path.

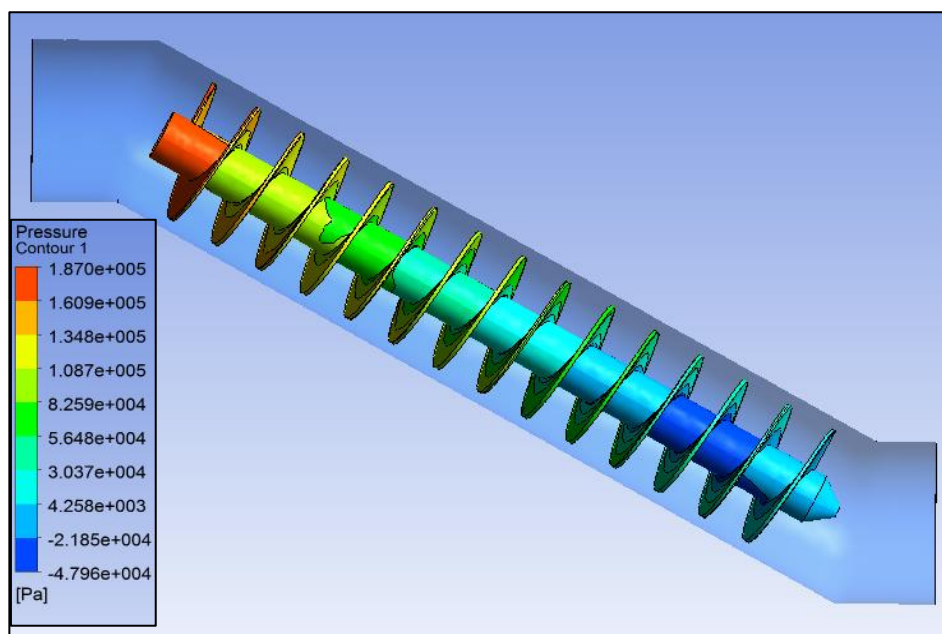


**Figure 4.3:** Pressure contour view at the screw runner blade

(Source: ANSYS CFD-Post result)



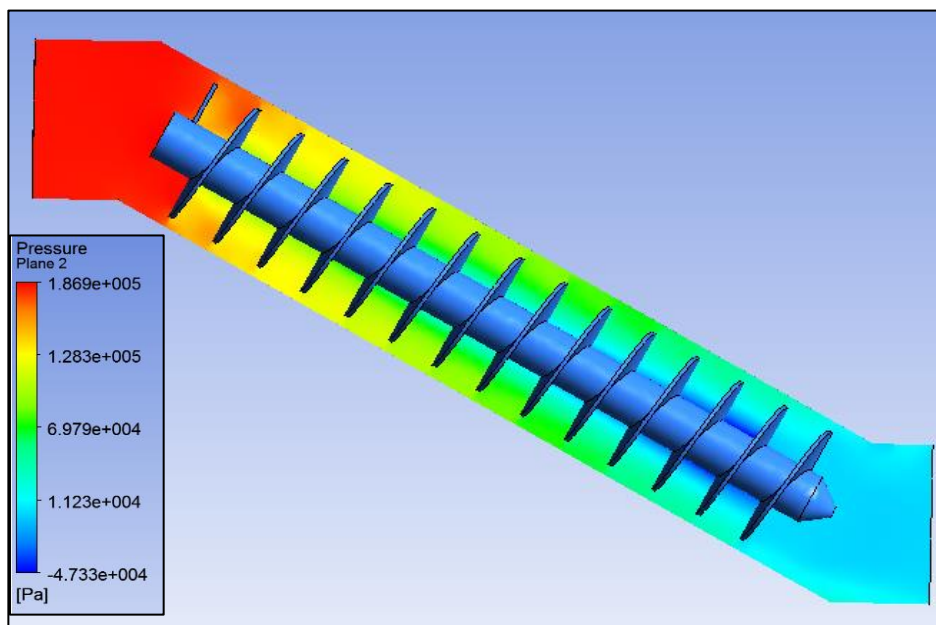


**Figure 4.4:** Pressure plane view at the screw runner blade

(Source: ANSYS CFD-Post result)

#### 4.4 Pressure Distribution on the 14 Screw Runner Blades

In this study the pressure behavior of the blade structure was observed. The simulation was performed with using 14 screw runner turn with the water path length of 6.8 meters and determined dimension of the screw blade. The flow was modeled using ANSYS-CFX solver according to the parameter stated. Based from the simulation, the result based from figure 4.5 shows that the pressure distribution on the first screw runner turn obtained the highest pressure value which was 187000 Pa. While the lowest pressure value obtained was -21850 Pa which situated at the end screw runner turn of the blade. As for the overall observation, the pressure distribution value decreases as the flow decline.

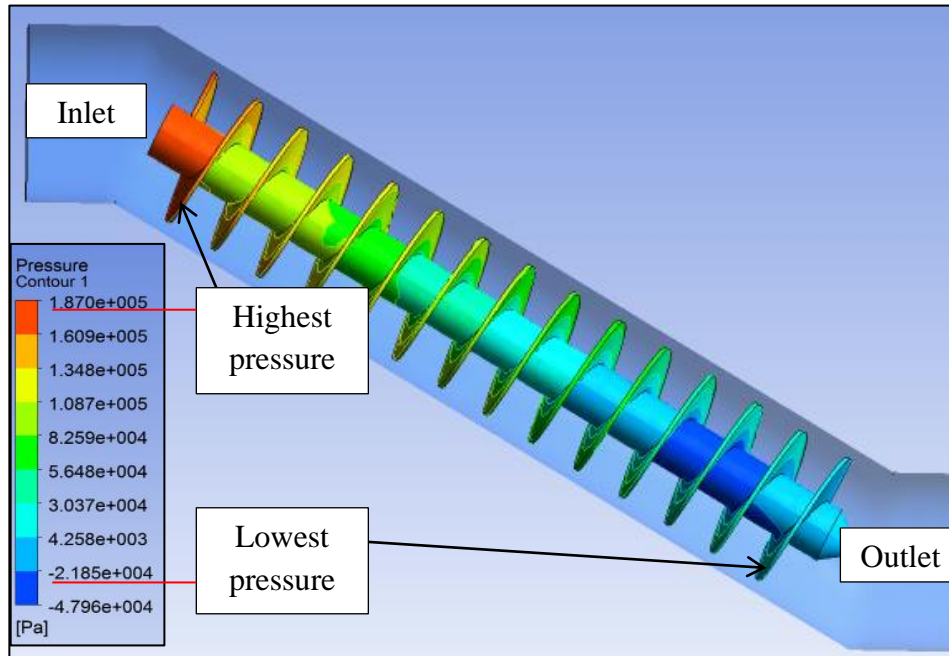


**Figure 4.5:** 14 helical blade pressure contour views

(Source: ANSYS CFD-Post result)

For reviewing more detailed pressure distribution at the blade structure, desired area on the blade structure was selected. Figure 4.6 shows the selected area were at the leading edge, blade tip and blade surface.

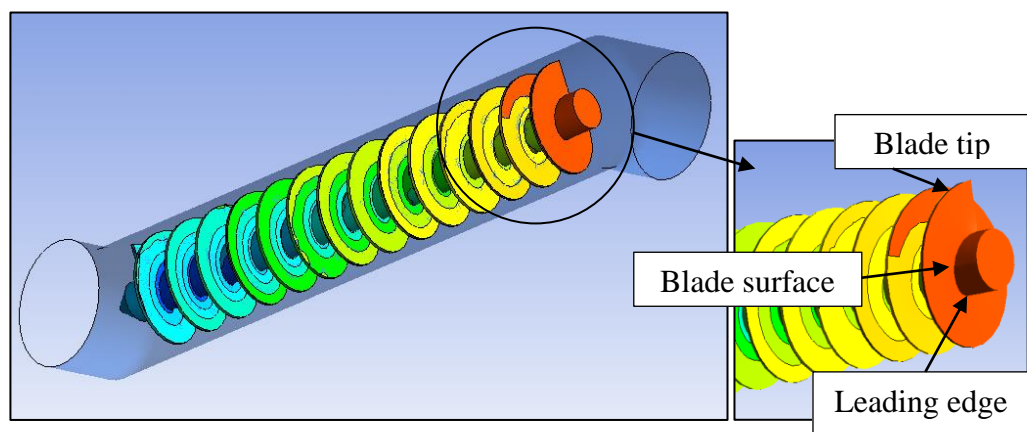


**Figure 4.6:** Location of leading edge, blade tip and blade surface

(Source: ANSYS CFD-Post result)

From the pressure distribution viewed, it was observed that the leading edge, blade tip and the blade surface located at the first screw runner turn experience the highest pressure value which at 187000 Pa. Figure 4.7 shows the plotted pressure distribution at the leading edge, blade tip and blade surface for the 14 screw runner blade structure.

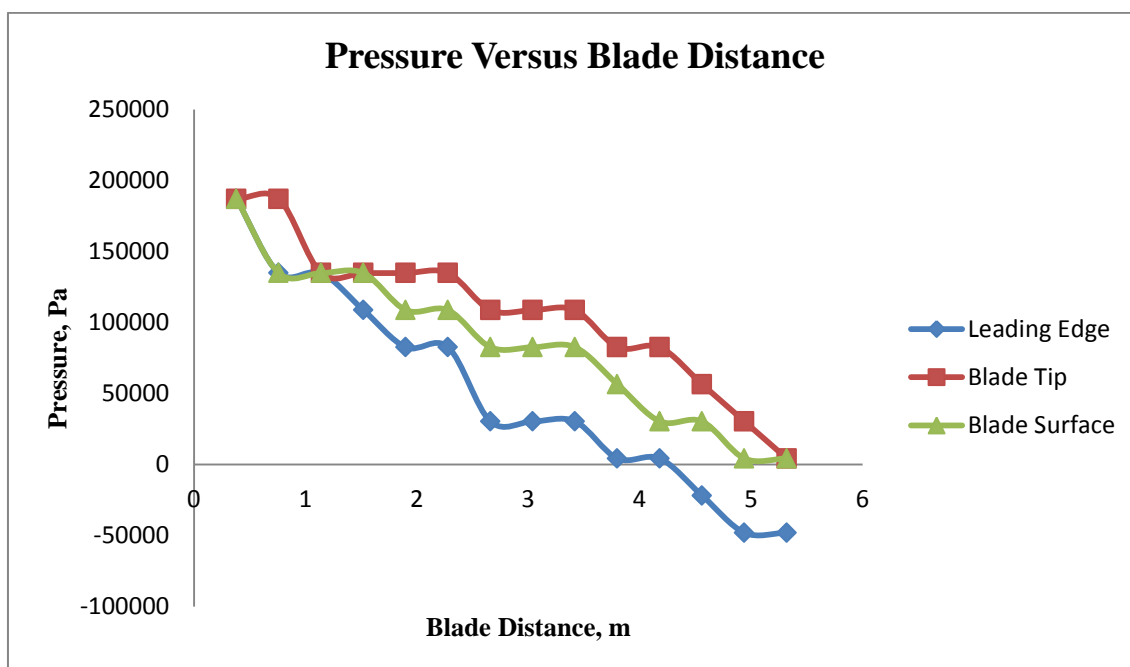


**Figure 4.7:** Graph of Pressure versus Blade Distance

Based from the plotted graph, it was observed that the blade tip of the screw runner blade experience higher pressure compared to the leading edge and also the blade tip. This was due to the position of the blade at the end structure of the blade. The high pressure reaction at the blade tip was due to the impact in rotation motion of the screw blade perpendicular with the impact of water that flow. This situation could cause the blade tip experience the high pressure. For both leading edge and blade surface, the pressure value experiences were lesser where the position was at the middle and also near to the turbine shaft. At this position, both structures were already immersed inside the water. Thus lower pressure value obtained at the leading edge of the screw runner blade.

#### 4.5 Velocity Distribution on the 14 Screw Runner Blades

For the observation of the velocity flow inside the flow path, the lower screw blade area was used as the blade only half immersed in the real situation. The velocity value then was selected at the leading edge area, blade tip area and also the blade surface area for obtaining the comparison based from figure 4.8.

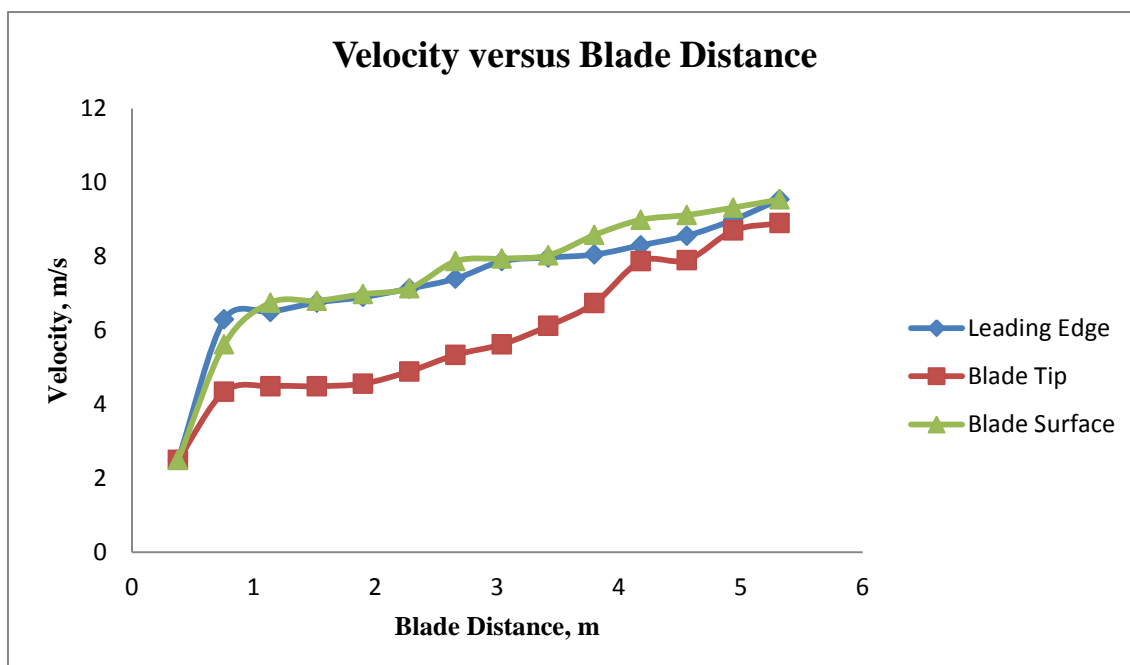


**Figure 4.8:** Graph of velocity versus blade distance

Based from the graph plotted, the velocity pattern obtain for all the area increases from the initial velocity which at 2.5 m/s. The velocity pattern at the blade tip area was lower compare to the leading edge area and also blade surface area. This was due to the surface water velocity in the real situation of water flow. On the other hand, the velocity value for both leading edge and blade surface area were higher where the area was under the water. The high velocity pattern observed caused from the underwater current flow as in real water flow.

#### 4.6 Coefficient of pressure on 14 Helical Screw Blades

Based from the pressure observe, the coefficient of pressure was taken for observing the value of specific pressure acted at the leading edge, blade tip and also blade surface. From the ANSYS software, we calculate the coefficient pressure value according to the general formulation express in equation 2.10. The new expression form equation 4.1 was for calculating the coefficient of pressure according to the software parameters.

Coefficient of Pressure,  $C_p$

$$C_p = \frac{\text{Total Pressure}}{(0.5 * \text{areaAve(Density)}@in * \text{areaAve(Velocity)}@in ^2)} \quad (4.1)$$

Figure 4.9 shows the coefficient of pressure distribution on the plane view along the flow path.

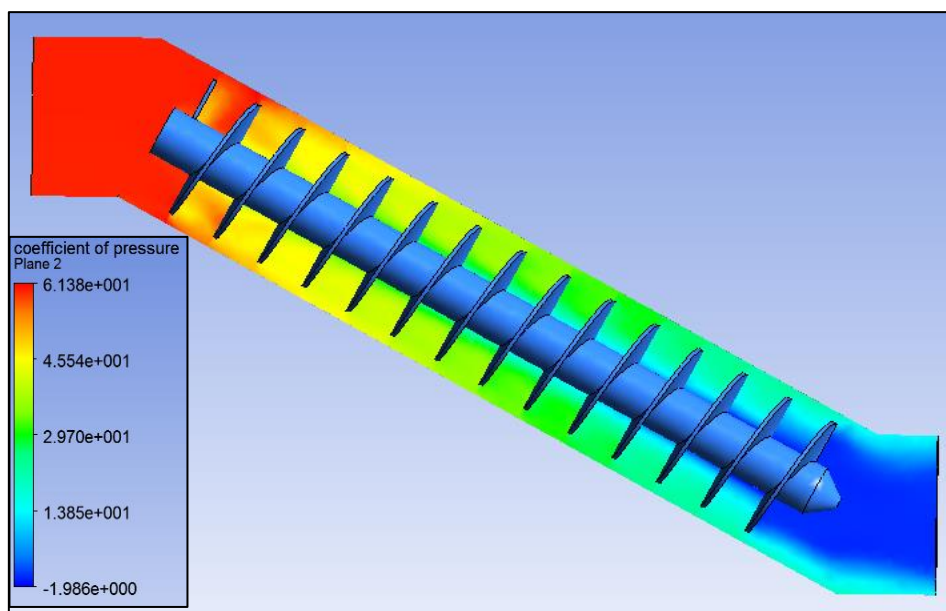


**Figure 4.9:** Coefficient of pressure distribution on plane view

(Source: ANSYS CFD-Post result)

While the coefficient of pressure for the blade structure was shown in figure 4.10. Contour was used for the observation at the blade structure.

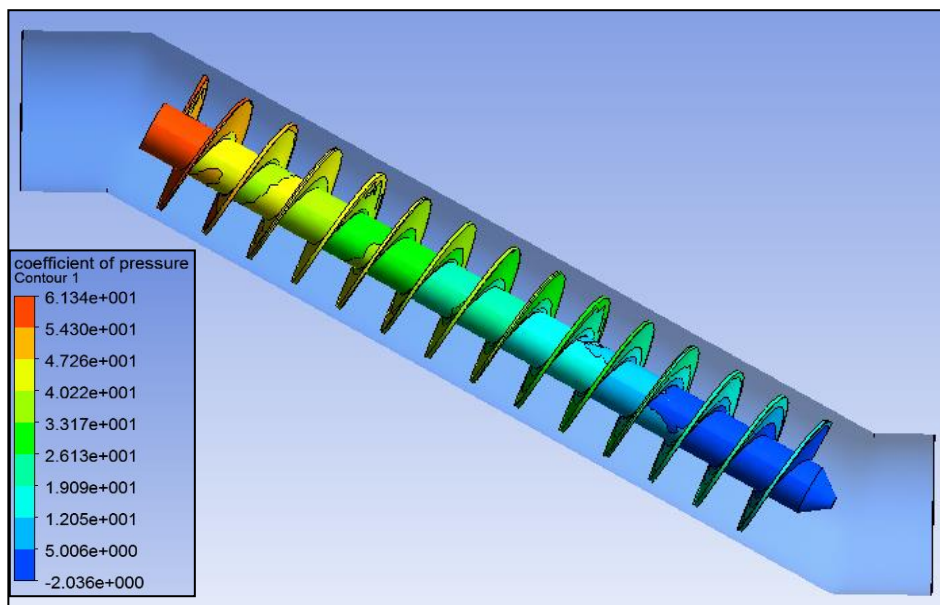


**Figure 4.10:** Coefficient of pressure contour view at the screw runner blade

(Source: ANSYS CFD-Post result)

In order to obtain the coefficient of pressure value, a specific point was plotted at the leading edge, blade tip and blade surface of the screw blade structure as shown in Figure 4.11.

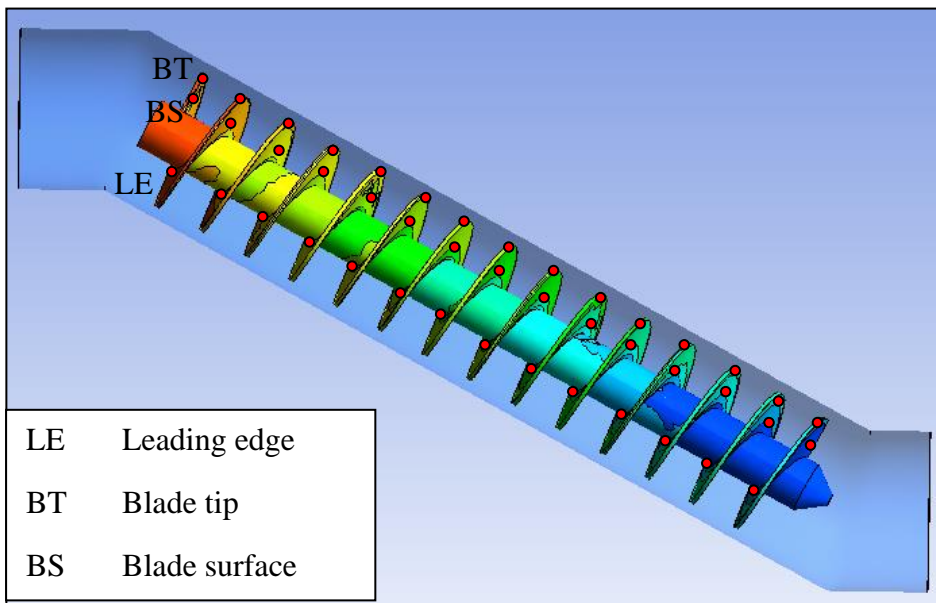


**Figure 4.11:** Plotted point at leading edge, blade tip and blade surface

(Source: ANSYS CFD-Post result)

Figure 4.12 shows the graph plotted for the coefficient of pressure at the leading edge, blade tip and blade surface.

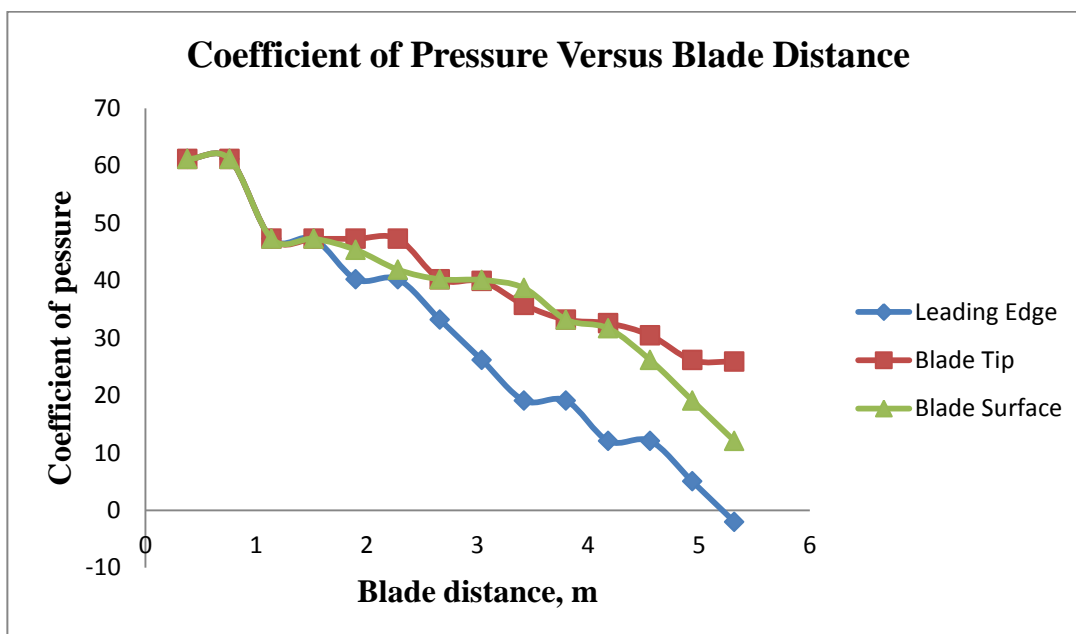


**Figure 4.12:** Graph of coefficient of pressure versus blade distance

Based from the graph plotted, it was observed that the highest coefficient of pressure value obtained was 61.134 at the water inlet of the screw blade. The leading edge, blade tip and also blade surface at the first screw runner turn experience the similar coefficient of pressure value. Thus, this can be said that the crack initiation was very critical at the first screw runner turns. For the observation of the coefficient of pressure on each of the targeted area, the blade tip shows the higher coefficient value compare to leading edge and blade surface. The lowest coefficient of pressure value for the blade tip was 25 while the blade surface was 12 and leading edge -2.036.



## **CHAPTER 5**

### **CONCLUSION**

#### **5.1 Introduction**

In this chapter will be discussed about the conclusion of the simulation done according to the crack initiation on the screw blade structure.

#### **5.2 Conclusion**

As for conclusion, the computational tool was able to solve the complex numerical problem related with the research of crack or erosion prediction on the Archimedes screw blade. The Archimedes screw blade can consume higher efficiency even though the blade was been implemented in low head hydro power. With the aid of the computational option provided, the simulation of the fluid flow on Archimedes screw blade can be perform with similar condition as in real picture of the working turbine.

Based from the simulation result, the visual view of the flow reaction was obtained on the Archimedes screw blade structure and also the flow path. The initiation of erosion pattern on the screw blade structure can be predicted to be occurred at the first screw blade turn. For the detailed viewed, the leading edge, blade tip and also blade surface at the first screw blade turn experience the highest pressure value which at 187000 Pa. For the overall viewed of the pressure distribution at 14 screw runner blade structure, the result shows that the blade tip experiences the highest pressure comparing to the leading edge and blade surface. This can conclude that the initiation of crack will be firstly initiate at the blade tip structure.

The other result shows that the highest coefficient of pressure value obtained was 61.134 at the first screw runner blade. The blade tip experiences the highest coefficient value comparing to the leading edge and also the blade surface. Thus, the result from both pressure and coefficient of pressure distribution shows that the prediction of crack will occurred at the blade tip area first. Even so, the crack initiation was considered to be in long period of time because of the slow rate of water velocity of the river water.

### **5.3 Recommendations**

As for the recommendation, in order to obtain the more accurate analysis result, the simulation of the screw blade must be done in half immersed and in rotating motion condition. The visual result from the rotating blade simulation can obtain the more specific pressure and coefficient of pressure distribution acted at the blade structure. The half flow simulation also can show the accurate prediction of particle size acted on the blade structure.

For other recommendation was conducting an experiment of the Archimedes screw runner hydro power in small scale. Based from the experiment, we can observe the fluid behavior acted from the flow motion inside the hydro power.

## REFERENCES

- Alkistis Stergiopoulou, Vassilios Stergiopoulos, 2012. Quo Vadis Archimedean Turbines Nowadays in Greece, in the Era of Transition
- Alessandro Corsini, Andrea Marchegiani, Franco Rispoli, Paolo Venturini, 2012. Predicting Blade Leading Edge Erosion in an Axial Induced Draft Fan
- B Thapa, M Eltvik, K Gjosater, O G Dahlhaug, 2012. Optimizing Runner Blade Profile of Francis Turbine to Minimize Sediment Erosion
- Chris Rorres, 1999. The Turn of The Screw: Optimal Design of an Archimedes Screw
- Dr. Vishnu Prasad, 2012. Numerical simulation for flow characteristic of axial flow hydraulic turbine runner
- Gerald Muller, James Senior, 2009. Simplified theory of Archimedean screws
- J.C. Marin, A. Barroso, F. Paris, J. Canas, 2008. Study of fatigue damage in wind turbine blades
- Miriam Flores, Gustavo Urquiza, José María Rodríguez, 2011. Fatigue Analysis of a Hydraulic Francis Turbine Runner
- R. Waddell, P. Bryce, 1999. Micro-Hydro System For Small Communities
- R.A. Saeed, A.N. Galybin, V. Popov, 2010. Modeling of flow-induced stresses in a Francis turbine runner
- S.E. Moussavi Torshizi, S.M. Yadavar Nikraves, A. Jahangiri, 2008. Failure analysis of gas turbine generator cooling fan blades
- Yoon Kee Kim, Qian Lu, Ho Seong Ji, Joon Ho Beak, Rinus Mieremet, Kyung Chun Kim, 2008. A Multi-Prong Study On Aerodynamic Characteristics of Archimedes Spiral-Type Wind Turbine Blade

**APPENDIX A**

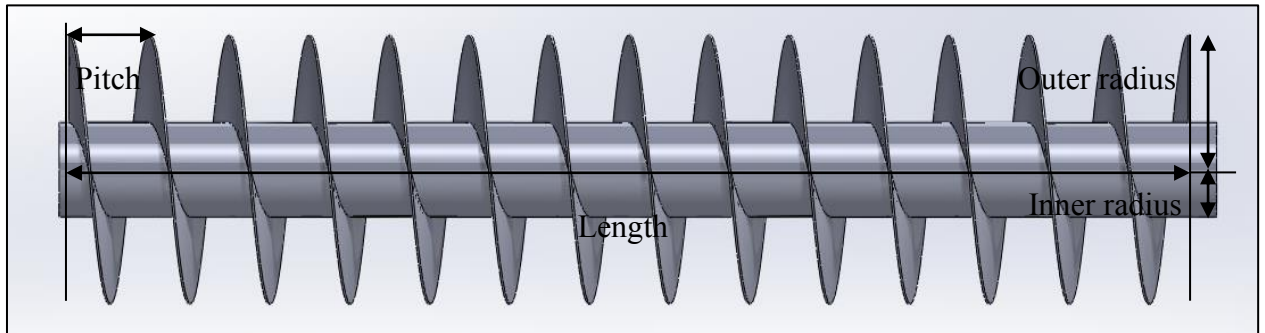


Figure 1A: Archimedes screw blade parameter labeled

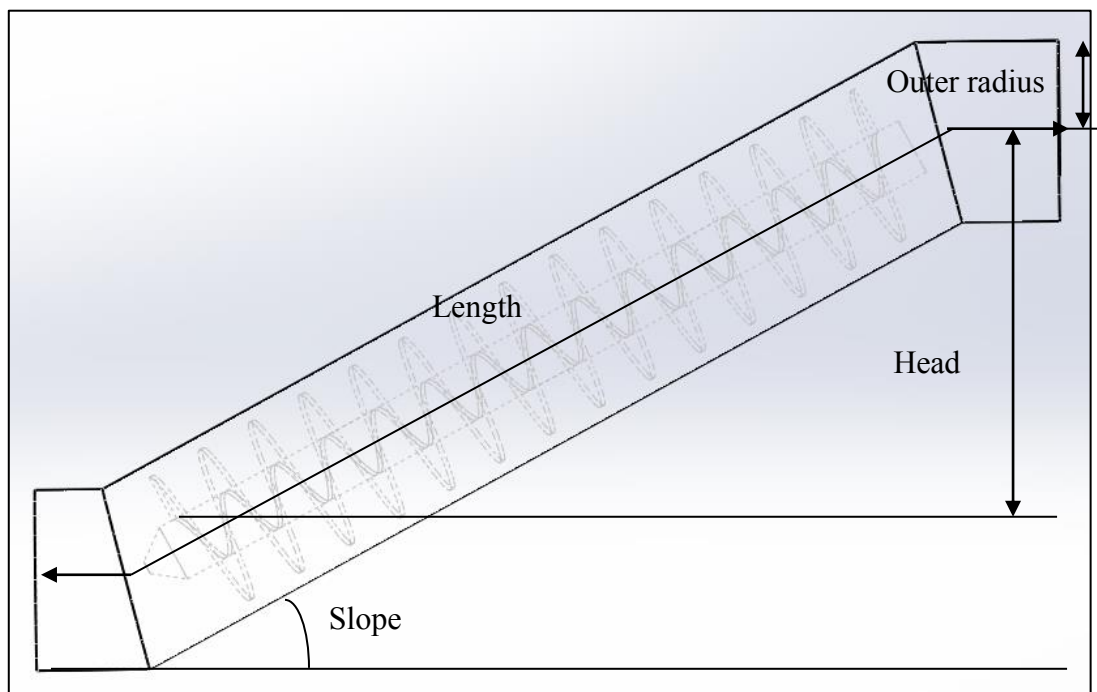


Figure 2A: Flow path parameter labeled

## EXAMINER'S DECLARATION

I certify that the project entitled "Predicting Crack Pattern on Archimedes Screw Runner Blade of Micro Hydro Power" is written by Ahmad Alif Bin Ahmad Adam. I have examined the final copy of this project and in my opinion, it is fully adequate in terms of scope and quality for the award of the degree of Bachelor of Engineering. I herewith recommend that it be accepted in partial fulfillment of the requirements for the degree of Bachelor of Mechanical Engineering

PROF MADYA DR. TUAN MOHAMMAD

YUSOFF SHAH TUAN YA

Examiner

Signature

### **SUPERVISOR'S DECLARATION**

I hereby declare that I have checked this project and in my opinion, this project is adequate in terms of scope and quality for the award of the degree of Bachelor of Mechanical Engineering.

Signature : .....

Name of Supervisor : MR MUHAMMAD AMMAR BIN NIK MU'TASIM

Position : LECTURER OF MECHANICAL ENGINEERING

Date : 26 JUNE 2013

## STUDENT'S DECLARATION

I hereby declare that the work in this project is my own except for quotations and summaries which have been duly acknowledged. The project has not been accepted for any degree and is not concurrently submitted for award of other degree.

Signature : .....

Name : AHMAD ALIF BIN AHMAD ADAM

ID Number : MC09017

Date : 26 JUNE 2013



Dedicated to my father, Mr. Ahmad Adam Bin Mohamed Yunus,  
my beloved mother, Mrs. Sharifah Binti Hassan  
and last but not least to all my fellow friends.

## ACKNOWLEDGEMENT

Alhamdulillah, praised to Allah, the most merciful for giving the chance, strength, inspiration and encouragement to complete this Final Year Project even there are some obstacles occurred. I would like to express my sincere appreciation to my main thesis supervisor, Mr. Muhammad Ammar Bin NikMu'tasim for his germinal ideas, invaluable guidance, continuous encouragement and constant support in making this research possible. He has always impressed me with his outstanding professional conduct, his strong conviction for science, and his belief that a bachelor program is only a start of a lifelong learning experience. Without his continuous support and interest, I would not have been able to complete this final year project successfully. I also sincerely thanks for the time spent proofreading and correcting my many mistakes.

I am also indebted to Universiti Malaysia Pahang (UMP) for providing internet and final year project lab facility. Special thanks also given to librarians UMP for their assistance in supplying the relevant literatures and are useful indeed.

I acknowledge my sincere indebtedness and gratitude to my parents for their love, dream and sacrifice throughout my life. I am also grateful to my fellow members for their supportive and helps that were inevitable to make this work possible. I cannot find the appropriate words that could properly describe my appreciation for their devotion, support and faith in my ability to attain my goals. I would like to acknowledge their comments and suggestions, which was crucial for the successful completion of this study.

## ABSTRACT

One of the fundamental studies of Micro hydro power with low head is the Archimedes screw runner. This research focuses on the study of behavior of fluid flow acting on the Archimedes screw runner blade and prediction of erosion pattern from fluid flow. The CAD model of the Archimedes screw blade was re-inversely design from past researcher. In order to determine the flow pattern, computational fluid dynamic, CFD was used to obtain the pressure distribution along blade structure. Analysis of three-dimensional with steady state flow was done with a standard k- $\epsilon$  as the turbulence model. The result obtained from pressure pattern shows that the highest value of coefficient of pressure obtained at the blade tip. This result shows that the prediction of crack may occur mostly at the blade tip. Further studies of blade design can be improved by reducing crack.

*Keywords: CFD, Archimedes screw runner blade, Micro hydro Power, Crack Pattern*

## ABSTRAK

Pelari skru Archimedes merupakan salah satu kajian asas kuasa micro hidro dengan kepala rendah. Kajian ini memberi tumpuan kepada kajian terhadap tingkah laku aliran cecair yang bertindak atas Archimedes skru bilah pelari dan ramalan corak hakisan daripada aliran cecair. Model CAD daripada bilah skru Archimedes adalah reka bentuk semula daripada penyelidik yang lepas. Dalam usaha untuk menentukan corak aliran, pengiraan cecair dinamik, CFD telah digunakan untuk mendapatkan corak tekanan sepanjang struktur bilah. Analisis tiga dimensi dengan aliran yang setabil telah dilakukan dengan  $k-\epsilon$  standard sebagai model turbulents. Keputusan yang diperolehi dari corak tekanan menunjukkan bahawa nilai tertinggi pekali tekanan didapati di hujung bilah. Keputusan ini menunjukkan bahawa ramalan keretakan boleh berlaku kebanyakannya di hujung bilah. Reka bentuk bilah pada kajian akan datang boleh diperbaiki dengan mengurangkan retak.

*Kata kunci: CFD, Bilah Skru Archimedes, Jana Kuasa Mikro Hidro, Corak Tekanan*

## TABLE OF CONTENTS

	<b>Page</b>
<b>EXAMINER’S DECLARATION</b>	ii
<b>SUPERVISOR DECLARATION</b>	iii
<b>STUDENT DECLARATION</b>	iv
<b>DEDICATION</b>	v
<b>ACKNOWLEDGEMENT</b>	vi
<b>ABSTRACT</b>	vii
<b>TABLE OF CONTENTS</b>	ix
<b>LIST OF TABLE</b>	xi
<b>LIST OF FIGURE</b>	xii
<b>LIST OF ABBREVIATIONS</b>	xiv
<b>NOMENCLATURES</b>	xv
<b>CHAPTER 1</b>	
<b>INTRODUCTION</b>	
1.1 Micro Hydro Power	1
1.2 Archimedes Screw Turbine	2
1.3 Problem Statements	3
1.4 Objectives	3
1.5 Scopes	3
<b>CHAPTER 2</b>	
<b>LITERATURE REVIEW</b>	
2.1 Introduction	4
2.2 Archimedes Screw Blade	4
2.2.1 Screw Blade Design	6
2.3 Governing Equation	8
2.4 Blade Optimum Rotation	10
2.5 Fatigue Crack	11
2.6 Crack Pattern Simulation	15

	2.7 Velocity of Pahang River	17
	2.8 Conclusion on the Literature Review	17
<b>CHAPETR 3</b>	<b>METHODOLOGY</b>	
	3.1 Introduction	18
	3.2 Flow Chart	18
	3.3 CAD Modeling	21
	3.4 Meshing (ANSYS CFX)	23
	3.5 Simulation	24
	3.5.1 Boundary Condition	25
	3.5.2 Imaginary Boundary	26
	3.6 Simulation of the Flow	27
<b>CHAPTER 4</b>	<b>RESULT AND DISCUSSION</b>	
	4.1 Introduction	29
	4.2 Result of Velocity Pattern	29
	4.3 Result of Pressure Pattern	31
	4.4 Pressure Distribution on the 14 Screw Runner Blade	32
	4.5 Velocity Distribution on the 14 Screw Runner Blade	35
	4.6 Coefficient of Pressure of the 14 Screw Runner Blade	36
<b>CAHPTER 5</b>	<b>CONCLUSION AND RECOMDENTADION</b>	
	5.1 Introduction	40
	5.2 Conclusion	40
	5.3 Recommendation	41
<b>REFFERENCES</b>		42
<b>APPENDICES</b>		43

**LIST OF TABLE**

<b>Table No.</b>	<b>Title</b>	<b>Page</b>
3.1	Dimension of the screw runner blade	22
3.2	Dimension of the flow path	23
3.3	Meshing detail of the flow path and screw runner blade	24
3.4	Default domain details	26
3.5	Inlet boundary and Outlet boundary details	27

## LIST OF FIGURE

<b>Figure No.</b>	<b>Title</b>	<b>Page</b>
2.1	The structure of Archimedes screw turbine	5
2.2	(a) Idealize Archimedes screw side and plan view (b) Hydrostatic pressure wheel (c) Force acting on individual screw blade	6
2.3	General external and internal parameter of Archimedes screw	7
2.4	CAD model for Archimedes screw	8
2.5	The theoretical efficiency as function of sloe angle and number of helical turns	11
2.6	Analysis using of the Francis turbine using computer simulation (b) Real image of the crack occurrence at the Francis turbine	12
2.7	(a) The crack propagation on the wind turbine blade (b) The simulation of the pressure distribution on the wind turbine blade	13
2.8	(a) The microstructure of the crack initiation (b) the distribution of stress at the gas turbine blade	14
2.9	(a) The fluid flow visual from ANSYS on Francis turbine (b) The pressure distribution from ANSYS on Francis turbine	15
2.10	Imaginary space on ANSYS	16
3.1	Flow chart for Semester 1 FYP progress	19
3.2	Flow chart for Semester 2 FYP progress	18
3.3	(a) Wireframe view and (b) Hidden line visible view of the screw runner blade with flow path on SolidWork	21-22
3.4	Mesh structure of the flow path and screw runner blade	24
3.5	The boundary condition setup for the simulation	25
3.6	The imaginary boundary for water flow inlet and outlet	26
3.7	Velocity vector view at the flow path	28
3.8	Graph of velocity versus flow path distance	28



**LIST OF FIGURES**

<b>Figure No.</b>	<b>Title</b>	<b>Page</b>
4.1	Velocity distribution plane view at the flow path	30
4.2	Velocity vector view at the flow path	30
4.3	Pressure contour view at the screw runner blade	31
4.4	Pressure plane view at the screw runner blade	32
4.5	14 helical blade pressure contour views	33
4.6	Location of leading edge, blade tip and blade surface	33
4.7	Graph of Pressure versus Blade Distance	34
4.8	Graph of velocity versus blade distance	35
4.9	Coefficient of pressure distribution on plane view	36
4.10	Coefficient of pressure contour view at the screw runner blade	37
4.11	Plotted point at leading edge, blade tip and blade surface of the screw blade	37
4.12	Graph of coefficient of pressure versus blade distance	38

**LIST OF ABBREVIATIONS**

CAD	Computer Aided Design
CFD	Computational Fluid Dynamics
C <sub>p</sub>	Coefficient of Pressure
areaAve	Average area
LE	Leading edge
BT	Blade tip
BS	Blade surface

**NOMENCLATURES**

kW	Kilo Watt
$\rho$	Density of fluid
t	Time
$\sigma$	Normal Stress for the momentum equation
$\tau$	normal viscous stress for the momentum equation
k	Kinematic energy
$\varepsilon$	Dissipation energy
S	Modulus of the mean rate-of-strain tensor
$\Delta P$	Pressure Difference
W	Blade surface velocity
$\Lambda$	Pitch
$R_o$	Outer radius
$R_i$	Inner radius
N	Number of blade revolution
L	Blade length
K	Slope
H	Head
Pa	Pascal
m	Meter
$^{\circ}C$	Degree Celsius